CO$_2$ flux characteristics of the open savanna and its response to environmental factors in the dry-hot valley of Jinsha River, China

Chaolei Yang[a,b,c,d], Yufeng Tian[a,b,c,d,*], Jingqi Cui[e], Guangxiong He[f], Jingyuan Li[e], Canfeng Li[a,b,c], Haichuang Duan[b], Zong Wei[a,b] , Liu Yan[a,b] , Xin Xia[a,b] ,Yong Huang[a,b], Aihua Jiang[a,b], and Yuwen Feng[g]

[a] Yunnan Provincial Observation and Research Station for Soil and Water Resources and Carbon Sequestration in the Alpine Gorge Area of Jinsha River, Chuxiong, 651400, China

[b] Kunming General Survey of Natural Resources Center, China Geological Survey, Kunming, 650111, China

[c] Technology Innovation Center for Natural Carbon Sink, Kunming, 650111, China

[d] Key Laboratory of Coupling Process and Effect of Natural Resources Elements, Beijing, 100055, China

[e] Institute of Space Weather, School of Atmospheric Physics, Nanjing University of Information Science and Technology, Nanjing, 210044, China

[f] Tropical Eco-Agriculture Research Institute, Yunnan Academy of Agricultural Sciences, Chuxiong, 651300, China

[g] Bazhong Meteorological Office of Sichuan Province, Bazhong, 636000, China

Correspondence to: Yufeng Tian (yufeng_tian818@126.com)

ABSTRACT: The dry-hot valley ecosystem of Jinsha River is a non-zonal special heat island habitat within the global temperate region. Revealing the CO$_2$ flux (Fc) changes and the response mechanisms of this ecosystem to environmental factors is crucial for accurately predicting the carbon (C) sequestration capacity of global terrestrial ecosystems, especially temperate ecosystems, under future extreme drought climate conditions. We focused on the open savanna, which is a core component of the Jinsha River dry-hot valley plant community, as our research subject. Using the static chamber method, we conducted long-term fixed-point observations of the Fc in the dominant grassy layer, explored the influence of different environmental factors on the Fc, and analyzed the trends of Fc changes in the open savanna under future extreme drought and low rainfall climate scenarios. The Fc of the open savanna exhibits distinct seasonal characteristics. During the dry season, it is in a C emission state, with a cumulative CO$_2$ emission of 1.3215 t·ha^{-1}. In contrast, during the rainy season, it shows significant C absorption characteristics, with a cumulative CO$_2$ absorption of 0.6137 t·ha^{-1}. The occurrence of extreme drought events in the study area has weakened the C absorption capacity of the open savanna, making it a weak C source with an annual cumulative CO$_2$ emission of 0.7078 t·ha^{-1}·a^{-1}, indicating a C-neutral feature. The main environmental factors affecting the net ecosystem exchange (NEE) variations in the open savanna across different seasons were different, but overall, soil water content was the key environmental factor controlling NEE. The response mechanisms of NEE to changes in different environmental factors were generally similar, with the NEE being at its minimum when located at the threshold of

environmental factors. When environmental conditions exceed or fall below this threshold, the C emissions of the open savanna will both increase. As the frequency and severity of future extreme droughts continue to rise, the C emissions from the open savanna in the study area will also continue to increase.

Key words: dry-hot valley of Jinsha River; open savanna; static chamber method; CO_2 flux; environmental factors

1 Introduction

Since the industrial revolution, human economic and social progress heavily relied on fossil energy consumption. The excessive emissions of greenhouse gases such as CO_2 have been considered to be the main cause of increased atmospheric CO_2 concentration and global warming (Sha et al., 2022; Wang et al., 2023).The terrestrial ecosystem can absorb about 15.0%–30.0% of anthropogenic CO_2 emissions per year, and the C neutrality capacity index reaches 27.14% (Green et al., 2019; Bai et al., 2023; Liu et al., 2023; Zeng et al., 2023). This makes it a significant C sink (Piao et al., 2018). With the intensification of global climate change, predicting the future C sequestration potential of terrestrial ecosystems will be of significant importance for formulating climate change adaptation strategies. However, due to the potential changes in precipitation patterns and rising temperatures caused by global climate change, the frequency and intensity of extreme climate events, especially high-temperature and drought events, are expected to continue to increase over the next few decades (IPCC, 2021). This will have profound impacts on the carbon source/sink structure of terrestrial ecosystems, particularly on the carbon cycle processes and their response mechanisms, making them more complex (Huang et al., 2024). This significantly hinders researchers' further in-depth understanding and accurate prediction of the carbon budget characteristics of terrestrial ecosystems under future climate change.

The global distribution of the savanna ecosystem is primarily determined by climate, fire, and anthropogenic disturbance (Williamson et al., 2024), covering approximately 1/6 of the Earth's land area (Grace et al., 2006). This ecosystem's structure and vegetation community composition are significantly influenced by hydrological conditions and are mainly composed of grass, with sparse distribution of trees and shrubs (Yu et al., 2015; Lee et al., 2018; Jin et al., 2019; Zhang et al., 2019; Hoffmann, 2023; He, et al., 2024). Being a significant component of the world's vegetation, the savanna's primary productivity accounts for about 30.0% of the primary production of all terrestrial vegetation, which has significant impacts on global material cycling, energy flow, and climate

change (Grace et al., 2006; Peel et al., 2007; Dobson et al., 2022). Due to the specific hydrothermal conditions, the F_c of the savanna ecosystem has significantly different characteristics in the dry season and the rainy season, with carbon absorption predominantly occurring during the rainy season, while the dry season is marked by a weak carbon source or sink feature (Grace et al., 2006; Millard et al., 2008; Livesley et al., 2011; Fei et al., 2017a). Additionally, the most savanna ecosystems globally demonstrate C sequestration features, with only a few exhibiting characteristics of C emissions, with the NEEvarying from around –3.87 to 1.28 t C·ha^{-1}·a^{-1} (Fei et al., 2017b).

The savanna ecosystem in China is mainly manifested as the ecological landscape of the valley-type sparsely shrub-grass vegetation distributed in the special geographical unit of the dry-hot valley. The ecosystem is characterized by a scarcity of woody plants, with the dominant herbaceous layer, i.e., the open savanna, being the core component of the plant community (Jin et al., 1987; Shen et al., 2010). It is also known as valley-type savanna vegetation and mainly concentrated in the Yuanjiang (YJ), Nu River, and Jinsha River (JS), and their tributaries in southwest China. The valley-type savanna ecosystem in China differs from other tropical savanna ecosystems. Located in the temperate zone within the global climatic zones, it represents a non-zonal special hot island habitat that has evolved from the global temperate humid climate zone (Zhang, 1992). The ecosystem has a relatively high average annual temperature and a significant potential evapotranspiration, which far exceeds the rainfall, making the issue of ecological drought particularly prominent. It is an ideal natural site for studying the carbon cycling process of terrestrial ecosystems under conditions of dry and high-temperature climates. Under the backdrop of intensifying global climate change, effectively revealing the carbon source/sink pattern and its influencing factors of the valley-type savanna ecosystem is of great scientific significance for profoundly understanding the impact of future extreme climate environments on the carbon sequestration function of terrestrial ecosystems, particularly those in temperate zones.

However, at present, there is a scarcity of research on the carbon source and sink characteristics of the Chinese valley-type savanna ecosystem (Fei et al., 2017a；Yang et al., 2020). In particular, open savanna, as the core component of the plant community in this ecosystem (Jin et al., 1987; Shen et al., 2010), their F_c can significantly impact the entire ecosystem and the surrounding areas' carbon balance even with minor dynamic changes. Nevertheless, there is still a research gap in studying the F_c changes and related influencing mechanisms, with open savanna serving as the observation object. We selected the the dry-hot valley of JS, the largest valley in China by area, as the study area, and took the open grasslands within it as the research object, using the static chamber method to observe the F_c of the dominant herbaceous layer.The aim is to clarify the dynamic

characteristics of open savanna F_c and its correlation with environmental factors, quantitatively assess the annual F_c, and attempt to address the trends of F_c changes under future drought and low precipitation climate scenarios. Hoping to provide scientific references for a deeper understanding of the key processes of carbon cycling in terrestrial ecosystems under arid and high-temperature climate conditions and for accurately predicting the carbon sequestration capacity of terrestrial ecosystems under extreme climate conditions.

2 Data and methods

2.1 Observation sites

All observational data were derived from the Jinsha River Field Observation Station (26°4'6.24" N, 101°49'41.68" E), whose test site is situated in the Shikanzi Daqing River Basin on the west bank of JS (Fig. 1), with a representative savanna ecological landscape. The elevation of the basin is 1200–1800 m, falling within the realm of the southern subtropical dry-hot monsoon climate, with the characteristics of drought, high temperature and less rain. The annual average temperature is 22.93°C, with daily maximum temperatures reaching over 43.00°C. The region has distinct rainy season (June to October) and dry season (November to May of the subsequent year), and the annual precipitation is 428.50 mm, with over 90.0% of the precipitation concentrated in the rainy season. The annual evaporation rate is high, typically 3–6 times the annual precipitation (He et al., 2000). The vegetation community is primarily dominated by herbs, with sparse woody plants. Herbaceous plants are mainly *Heteropogon contortus* (Linn.) Beauv., *Eulaliopsis binate* (Retz.) C. E. Hubb, *Cymbopogon goeringii* (Steud.) A. Camus, *Eulalia speciosa* (Debeaux) Kuntze, and so on. The shrubs include *Phyllanthus emblica* L., *Pistacia weinmannifolia* J. Poisson ex Franch, *Quercus franchetii* Skan, *Quercus cocciferoides* Hand. –Mazzz, and *Dodonaea viscosa* (L.) Jacq., etc.

2.2 Data source

2.2.1 Micrometeorological Factor Observation

The micro-meteorological factors were continuously monitored in real-time by the DL3000 small automatic meteorological observation system deployed in the test site of the observation station. The observation time began on January 12, 2023, and the observation indexes included air temperature (Ta), relative humidity (RH), soil temperature (Ts), soil water content (SWC), soil conductivity (SC), precipitation (P), wind speed (Ws), wind direction (WD), and photosynthetically active radiation (PAR). The average value of the environmental factors observation data for 5 minutes, 30 minutes, and 24 hours are automatically recorded through the CR1000X data logger. The specific meteorological observation system sensor equipment information is listed in Table 1.
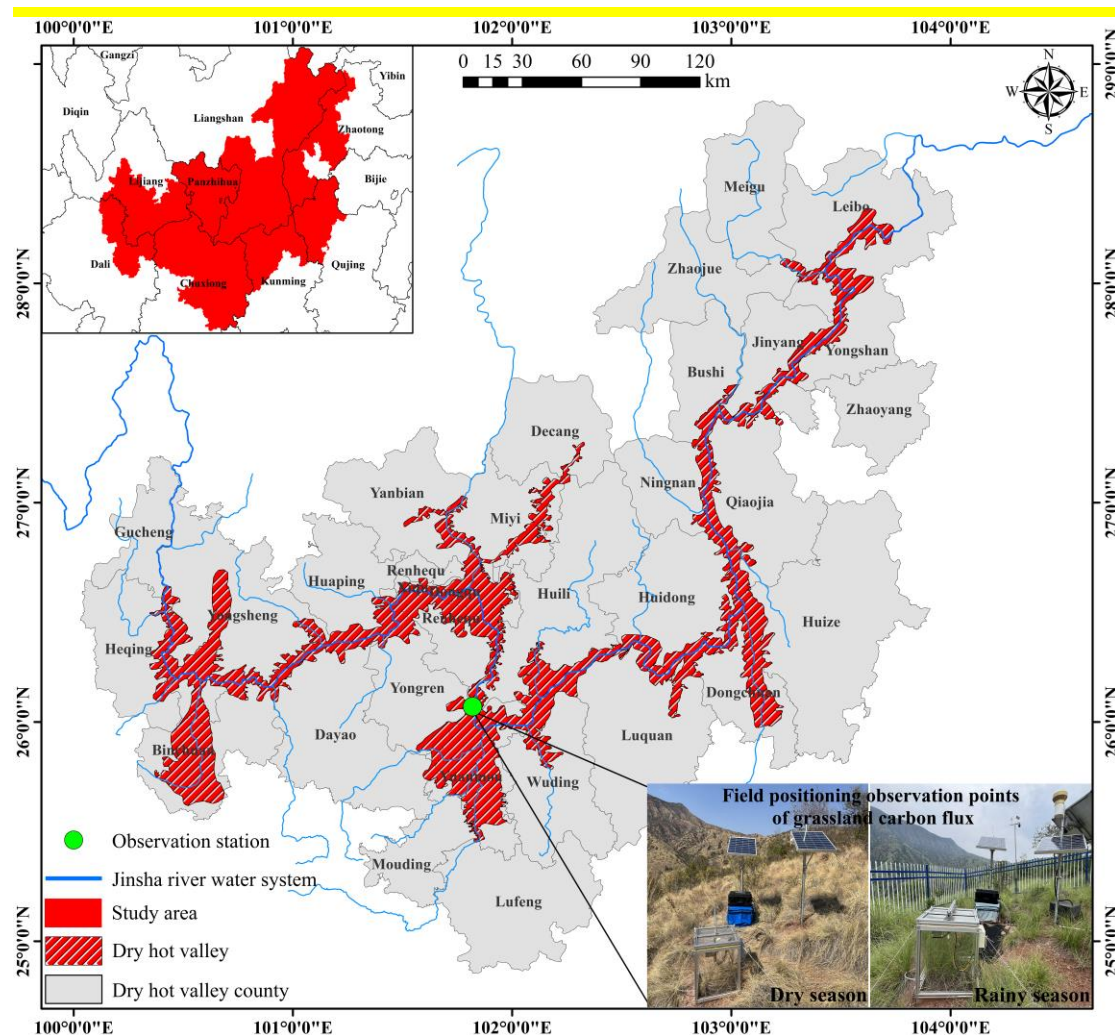
2.2.2 CO_2 flux observation

In order to ensure the representativeness of the observation plots and the spatial integration of the observation data, the typical grassy layer plots with small micro-habitat differences were selected in the test site of the observation station to lay out and install static assimilative boxes for positioning observation. The observation point is about 10 meter away from the automatic meteorological observation system. The observation time began at 3:05 PM on March 3, 2023, and ended at 10:50 AM on November 1, 2023. The bottom area of the assimilative box is 0.25 m^2, and the volume in the box is 125 L. The whole box is composed of transparent organic glass. There are two sets of fans in the box, which can fully mix the gas evenly. The height of the base is 8cm, embedded in the underground soil is 5 cm, and the aboveground part is 3 cm. The NEE was mainly measured by the CARBOCAP ® C dioxide sensor GMP343 of Vaisala Company. The diffusion probe of the sensor can effectively reduce the measurement error caused by the pressure difference of the pumping system. It has the characteristics of flexibility and high precision and is widely used in ecosystem CO_2 monitoring (Harmon et al., 2015). The top cover of the assimilative box can be

5

automatically opened and closed, and the time of a single complete measurement cycle is 15 minutes. Before the measurement, the top cover of the assimilative box will be automatically opened, so that the gas in the box and the surrounding air are mixed evenly, and the time is 5 minutes. Then the top cover of the box is automatically closed to a closed and stable state, the fan starts, and the gas change in the box is measured. The measurement and recording time is 10 minutes, so repeated.

Table 1 Information of micrometeorological observation system.

Name of instrument	Manufacturer	Observation parameter	Height (depth) of installation (m)
Temperature and humidity sensor	Campbell	Ta (°C) and RH (%)	1.5
Photosynthetic effective radiometer	Campbell	PAR (μmol·m^{-2}·s^{-1})	1.5
Wind speed and direction sensor	Campbell	Ws (m/s) and WD (°)	1.5
Rainfall sensor	Campbell	P (mm)	1.5
Soil multi-parameter sensor	Campbell	Ts (°C), SWC (m^3 · m^{-3}), and SC (dS/m)	Soil horizon 0.1

2.2.3 Other data

The boundary data of the dry-hot valley was sourced from Deng (2022). The administrative boundary data (Xu, 2023a; Xu, 2023b) and river data (Xu, 2018) were sourced from the Resources and Environment Science Data Center (RESDC) from the Chinese Academy of Sciences.

2.2.4 Data processing

When the F_c is measured, the whole monitoring system will collect the original data of GMP343 at a speed of 2 Hz through the CR1000X data logger, and average the data collected within 5 seconds for statistical analysis (main scan interval). If the difference between the newly acquired data and the average value exceeds 8 times the standard deviation, it is classified as an outlier, and such data points are eliminated. The system performs linear regression fitting on the removed data and calculates the ecosystem CO_2 exchange capacity, goodness of fit, etc.

The ecosystem CO_2 exchange capacity is calculated by the formula (1):

$$F_c = \frac{V \times P_{av} \times (1000 - W_{av})}{R \times S \times (T_{av} + 273)} \times \frac{\partial_c}{\partial_t} (1)$$

where F_c represents CO_2 flux (μmol·m^{-2}·s^{-1}); V represents the volume of assimilative chamber (m^3); P_{av} represents the mean atmospheric pressure (kPa) inside the chamber during the observation period; W_{av} represents the partial pressure of water vapor inside the chamber during the observation period (mmol·mol^{-1}); R represents the atmospheric constant (8.314 J·mol^{-1}·K^{-1}); S represents the area of assimilative chamber (m^2); ∂_c / ∂_t represents the diffusion rate of CO_2 in the chamber; T_{av} represents the mean temperature (°C) inside the chamber during the observation period.

177   The linear regression method was employed to fit the CO_2 diffusion rate (∂_c / ∂) (formula 2).

178   This method is the basic method for measuring the CO_2 diffusion rate of most soil respiration and

179   is widely used (Wen et al., 2007):

180
$$c(t) = c + \frac{\partial_c}{\partial_t}t \ (2)$$

181   where $c(t)$ represents the CO_2 concentration within the assimilative chamber; t represents the

182   determination time; c represents the CO_2 concentration in the assimilative chamber when it is closed.

183   Taking into account the specific conditions of the study area, the recorded Fc data was

184   categorized into dry season (March 3rd–May 31st) and rainy season (June 1st–November 1st). Due

185   to the damage of the assimilative box from June 1st to August 6th and the lack of observation data,

186   considering the continuity of the data time series and the precision of the data, the dry season Fc

187   data is mainly based on the observation data from March 4th to May 31st, and the rainy season Fc

188   data is mainly based on the observation data from August 7th to October 31st. Quality control was

189   conducted on the raw data to remove invalid NAN values and abnormal data (the abnormal data

190   mainly consisted of negative values during the dry season and negative values at night during the

191   rainy season). Utilizing the research results from Zhao et al. (2020), missing data points with a time

192   difference of under 3 hours are filled in using linear interpolation. For data with a missing duration

193   of more than 3 hours, interpolation is mainly performed by distinguishing between daytime and

194   nighttime periods. Among them, the data of daytime in the rainy season were interpolated by

195   formula (3) rectangular hyperbolic model (Ruimy et al., 1995) to simulate the relationship between

196   NEE and PAR. The missing data of the rainy season at nighttime and the dry season were

197   interpolated by the multiplicative model (4) of the response of ecosystem respiration to Ts and SWC:

198
$$NEE_{daytime} = R_{daytime} - \frac{A_{max} \times \alpha \times PAR_{daytime}}{A_{max} + \alpha \times PAR_{daytime}}(3)$$

199   where $NEE_{daytime}$ represents the NEE during the daytime ($\mu mol \cdot m^{-2} \cdot s^{-1}$); A_{max} represents the

200   maximum photosynthetic rate ($\mu mol \cdot m^{-2} \cdot s^{-1}$); α represents the apparent quantum efficiency

201   ($\mu mol \cdot mol^{-1}$); $R_{daytime}$ represents the daytime ecosystem respiration rate ($\mu mol \cdot m^{-2} \cdot s^{-1}$); $PAR_{daytime}$

202   represents the PAR during the daytime ($\mu mol \cdot m^{-2} \cdot s^{-1}$).

203
$$ER = a \times e^{\beta T_s} \times SWC^C(4)$$

204   where ER represents the ecosystem respiration rate ($\mu mol \cdot m^{-2} \cdot s^{-1}$); α, β and c represents the fitting

205   parameters; Ts and SWC are shown in Table 1.

206   The vapor pressure deficit (VPD) is calculated by formula (5) (Campbell et al., 2012):

207
$$VPD = 0.61078e^{\frac{17.27Ta}{Ta+237.3}}(1 - RH)(5)$$

7

208 where *RH* and *Ta* are shown in Table 1.

3 Analysis of the effect

3.1 Dynamic changes in environmental factors

Utilizing the observational data of micrometeorological factors, the dynamic attributes of environmental factors such as Ta, VPD, RH, P, Ws, PAR, Ts and SWC. It can be seen that these environmental factors showed a high degree of seasonal characteristics, especially the P and SWC were the most obvious. Among them, the P in the rainy season was 400.80 mm, mainly concentrated in August (142 mm). The precipitation frequency was 17 times, and the SWC changed between 0–0.19 $m^3 \cdot m^{-3}$ (Fig. 2a and 2b). The minimum RH was 20.65% and the maximum was 94.10%, showing a strong response relationship with P. The VPD fluctuated between 0.11–4.13 kPa, and its value decreased significantly after May, which was related to the increase of P and RH in the rainy season (Fig. 2a and 2c). During the observation period, the PAR varied from 52.28–860.59 $\mu mol \cdot m^{-2} \cdot s^{-1}$, influenced by weather conditions and displaying significant fluctuations (Fig. 2d). From different seasons, the daily average of PAR in the dry season (476.50 $\mu mol \cdot m^{-2} \cdot s^{-1}$) exceeded that of the rainy season (432.79 $\mu mol \cdot m^{-2} \cdot s^{-1}$). During the dry season, the mean Ta was 23.04°C, while in the rainy season, it averaged 25.38°C. The difference was small. Secondly, the highest and lowest values of Ta appear in May of the dry season. The range of Ta and Ts was 8–34.52°C and 11.58–36.97°C, respectively. The seasonal variation characteristics of the two were similar, but the Ts was significantly higher than the Ta, and the change time lags behind the Ta (Fig. 2e). In terms of changes in Ws characteristics, the highest value of Ws appeared in March, reaching 2.93 $m \cdot s^{-1}$, and the lowest value appeared in June, which was 0.57 $m \cdot s^{-1}$. The daily average Ws was the highest in February, which was 1.90 $m \cdot s^{-1}$, and the lowest in August, which was 0.99 $m \cdot s^{-1}$. The Ws decreased significantly after mid-July (Fig. 2f). Finally, it is particularly noteworthy that the annual P in the study area has been continuously decreasing in recent years (Fig. 3), especially in 2023, which recorded the lowest annual P since historical data has been recorded. It is a typical extreme drought event (Wang et al., 2025).
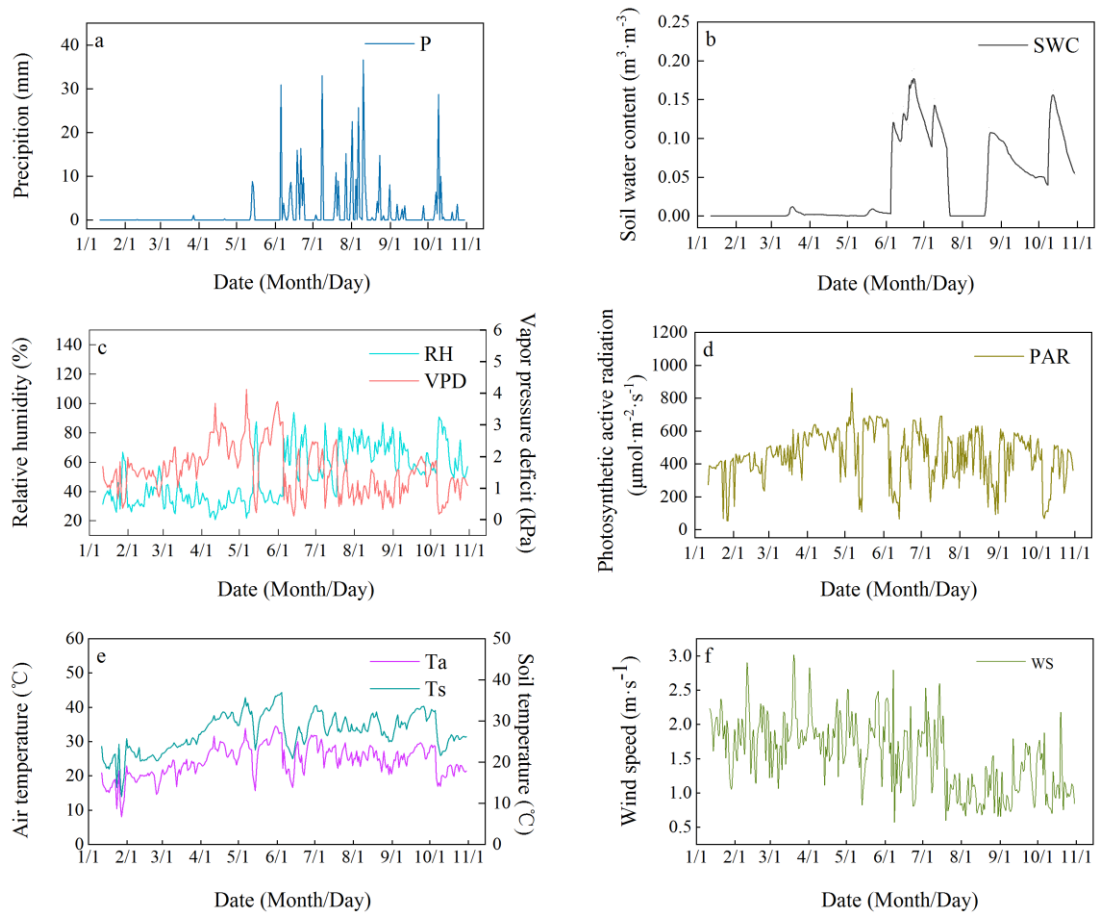
Figure 2 The variation characteristics of environmental factors in the study area.
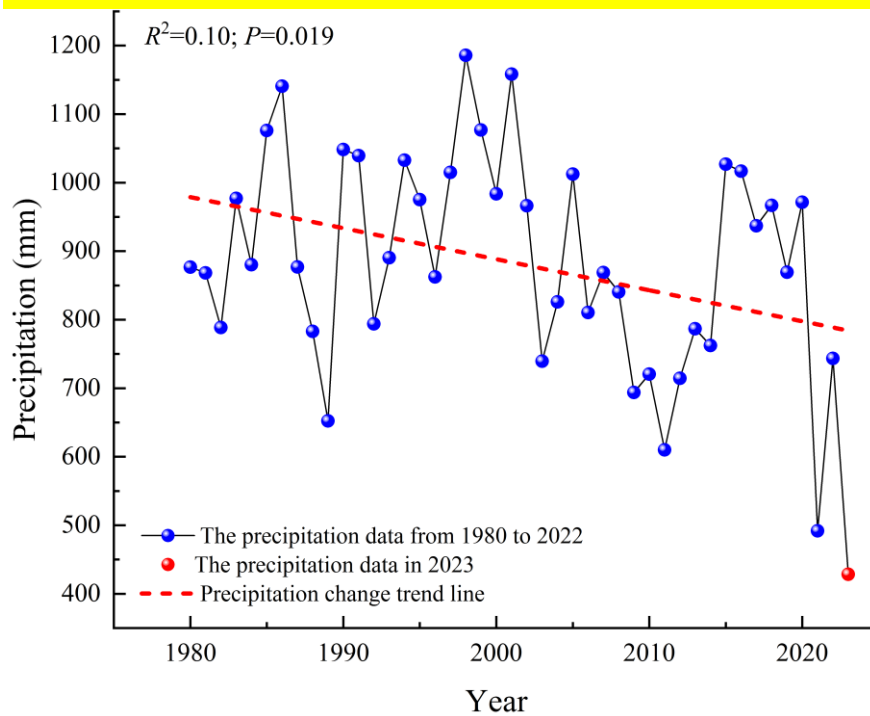

Figure 3 The precipitation changes in the study area from 1980 to 2023 (The precipitation data from 1980 to 2022 were collected from Yunnan Statistical Yearbook, and the precipitation data in 2023 were the measured data of Jinsha River Field Observation Station).

9

3.2 Diurnal variation of CO_2 flux

The F_c was positive, indicating a C emission state, throughout the entire diurnal variation process in the dry season. The diurnal variation showed a 'W'-type bimodal curve (Fig. 4a) of decreasing → increasing → decreasing → increasing, that is, the F_c was lower in the morning and afternoon, and the F_c was higher in the nighttime and noon, especially in April and May when this diurnal variation pattern was most pronounced. The lowest F_c values appeared in the morning (8:00−10:00) of each month, which were 0.1178 μmol·m^{-2}·s^{-1}, 0.1148 μmol·m^{-2}·s^{-1}, and 0.1397 μmol·m^{-2}·s^{-1}, respectively. The highest F_c value appeared in the evening (19:20) in March, which was 0.2158 μmol·m^{-2}·s^{-1}. In April and May, it appeared in the evening (13:35). They were 0.1148 μmol·m^{-2}·s^{-1} and 0.1397 μmol·m^{-2}·s^{-1}, respectively. During the dry season, the herbaceous plants in the study area were in a senescent state, and the open savanna was characterized solely by soil respiration. The study by Carey et al. (2016) found that in all non-desert biomes, soil respiration increases with rising soil temperature, however, beyond a certain threshold, the soil respiration rate decreases with further temperature increases. Therefore, we believe that the diurnal variation of F_c in the open savanna of the JS dry hot valley during the dry season primarily relates to the diurnal variation of temperature. From night to morning, the temperature gradually decreased, leading to a reduction in soil respiration and a decrease in F_c. It was not until around 10:00 AM that the temperature began to rise, increasing in the intensity of soil respiration and a continuous rise in F_c, reaching its peak. Subsequently, the soil respiration rate decreased with further temperature increases, and after about 5:00 PM, as the temperature gradually declined, the limitation on soil respiration weakened, and F_c gradually increased again.

The diurnal variation of the F_c was characterized by a 'U'-shaped single-peak curve, which was stable at night and decreased first and then increased during the day (Fig. 4b), during the rainy season. At about 7:35 in the morning, with the increase of PAR intensity, the photosynthesis of the herbaceous plants was continuously enhanced, and the F_c began to become negative. At this time, the open savanna changes from C emission at night to C absorption, forming the source of CO_2 absorption and reaching the maximum peak of C absorption at 10:00–14:00. Until about 17:20, the F_c becomes positive again. The open savanna transitions into a state of C emission, releasing CO_2 into the atmosphere. During the rainy season, the SWC was relatively high, and the increase in SWC had an inhibitory effect on the temperature sensitivity of soil respiration (Xiang et al., 2017). As a result, the F_c during the nighttime period remained relatively stable. The lowest F_c values appeared in the morning (10:00–12:00) from the diurnal variation of flux in various months, which were −1.4286 μmol·m^{-2}·s^{-1}, −1.3834 μmol·m^{-2}·s^{-1}, and −1.0278 μmol·m^{-2}·s^{-1}, respectively. The highest F_c

values appeared in the evening (18:35–18:50), which were 0.7584 $\mu mol \cdot m^{-2} \cdot s^{-1}$, 0.4959 $\mu mol \cdot m^{-2} \cdot s^{-1}$ and 0.5715 $\mu mol \cdot m^{-2} \cdot s^{-1}$, respectively.
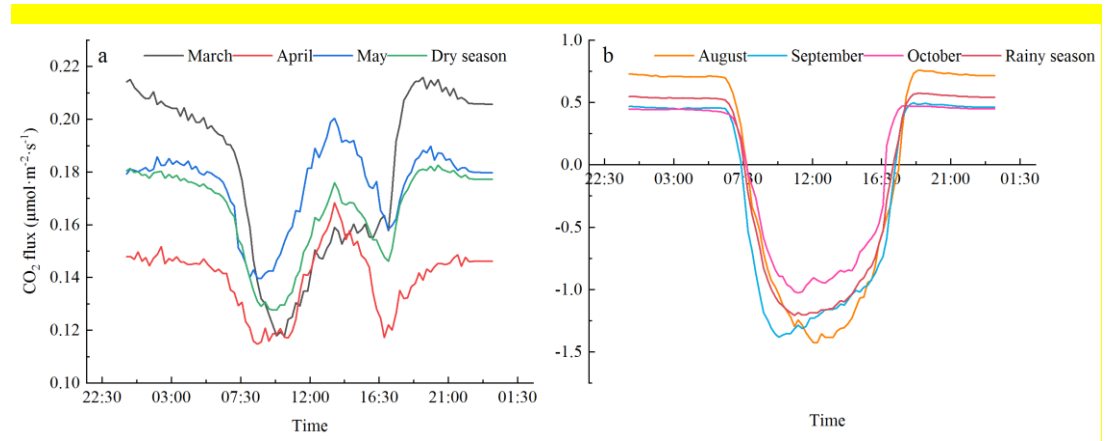

Figure 4 Diurnal variation characteristics of the Fc (a−dry season; b−rainy season).

3.3 Seasonal variation of CO_2 flux

From Fig.5, we can find that the seasonal variation of the Fc was evident. In the dry season, the ecosystem experiences severe drought and water scarcity, leading to poor growth of herbaceous plants, which is characterized by C emissions. The monthly cumulative CO_2 emission fluxes were 18.64 $g \cdot m^{-2}$, 15.96 $g \cdot m^{-2}$, and 20.64 $g \cdot m^{-2}$, respectively, displaying an initial decline followed by a rise. The CO_2 emission flux was the highest in May. The ecosystem has abundant P in the rainy season, the SWC is high, the herbaceous plants are in the growing season, and the photosynthesis capacity is significant, so it is characterized by the C sink function. The monthly cumulative CO_2 absorption fluxes were 6.42 $g \cdot m^{-2}$, 24.41 $g \cdot m^{-2}$, and 5.14 $g \cdot m^{-2}$, respectively, displaying a rise initially followed by a decline, and the C absorption capacity in September was the most significant.
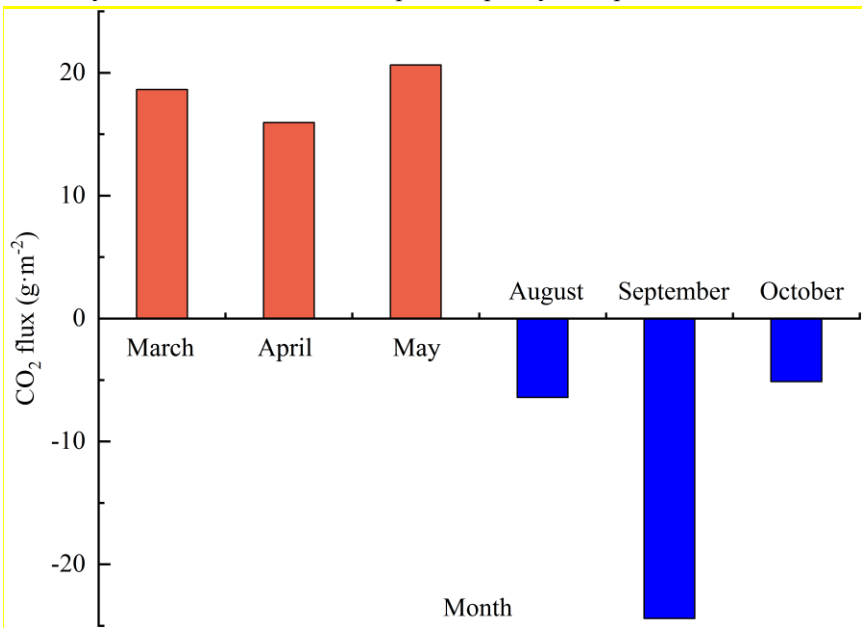

Figure 5 Monthly variation characteristics of the Fc.

11

289   The existing observation data were averaged and calculated respectively in this study, and they

290   were used as the daily mean F_c of the two seasons in the whole year. According to the days of the

291   dry season (213 days) and the rainy season (152 days) in the whole year, the dry season, rainy season,

292   and annual F_c of the open savanna were calculated. The findings indicated that the mean daily F_c

293   was 0.1632 $\mu mol \cdot m^{-2} \cdot s^{-1}$ in the dry season, and the cumulative CO_2 emission was 1.3215 $t \cdot ha^{-1}$. The

294   daily average F_c was –0.1062 $\mu mol \cdot m^{-2} \cdot s^{-1}$ in the rainy season, and the cumulative CO_2 uptake was

295   0.6137 $t \cdot ha^{-1}$. From the annual scale, the cumulative F_c of the open savanna was 0.7078 $t \cdot ha^{-1} \cdot a^{-1}$

296   (0.1926 $t\ C \cdot ha^{-1} \cdot a^{-1}$), making it a weak C source.

297   3.4 The relationship between CO_2 flux and environmental factors

298   3.4.1 Response of CO_2 flux to PAR

299   This study selected F_c data and micrometeorological observation data to analyze the

300   interrelations between F_c and environmental factors, as well as among different environmental

301   factors (Fig. 6 and 7). The research area belongs to a typical semi-arid region, where vegetation

302   growth and physiological processes are mainly regulated by temperature and moisture factors (Jiang

303   et al., 2007; Fei et al., 2017a). Therefore, when analyzing the influencing factors of ecosystem CO_2

304   flux, we mainly selected environmental factors including P, SWC, Ts, Ta, RH, PAR, and VPD for

305   Pearson analysis and quadratic regression analysis. No significant correlation between PAR and F_c

306   during the dry season was indicated by the results of the Pearson correlation analysis ($R^2 = 0.03$, P

307    $= 0.092$). Still, there was a strong negative correlation between PAR and F_c during the rainy season

308   ($R^2 = 0.33$, $P < 0.01$), and this relationship was more obvious in Fig. 6a. As a key environmental

309   factor driving plant photosynthesis, photosynthetically active radiation will directly affect the C

310   absorption rate of the open savanna and further affect the C budget pattern of the ecosystem. In the

311   rainy season, the F_c decreased with the increase of PAR, and the C absorption capacity increased

312   continuously, and the relationship between them could be expressed by formula (3). When PAR was

313   under 500 $\mu mol \cdot m^{-2} \cdot s^{-1}$ (Fig. 6b), the NEE of the ecosystem decreases rapidly with increasing PAR.

314   At the same time, the distribution of NEE with PAR was relatively concentrated. However, when

315   PAR was above 500$\mu mol \cdot m^{-2} \cdot s^{-1}$, the magnitude of the decrease in NEE with increasing PAR

316   gradually decreases, and the distribution of NEE with PAR was relatively scattered, indicating that

317   the F_c was also influenced by various other environmental factors present in the ecosystem when

318   solar radiation is high. These research findings align with those of previous studies carried out in

319   diverse grassland ecosystems (Zhao et al., 2007; Wang et al., 2015; Guo et al., 2022).
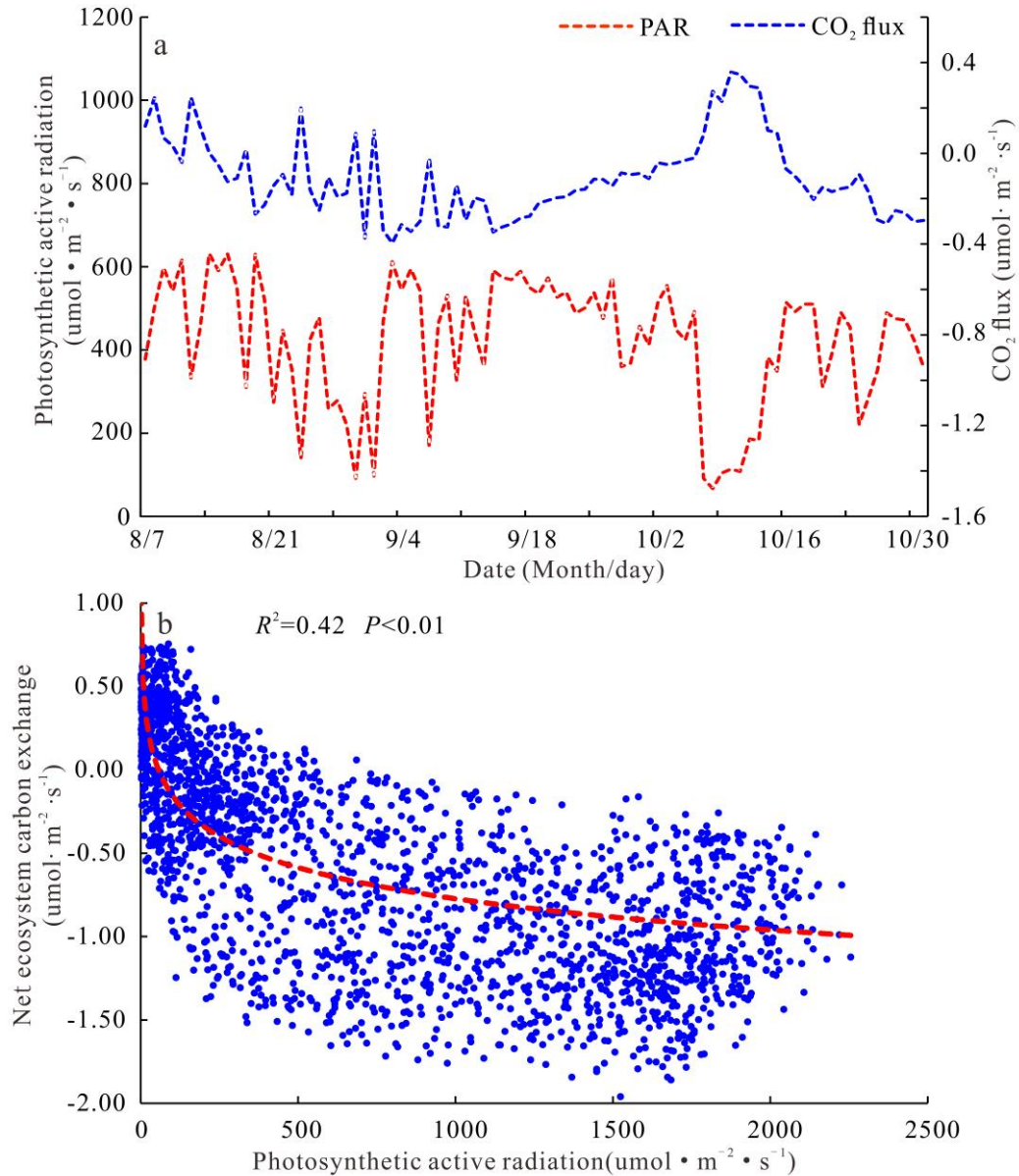
Figure 6 The correlation between PAR and Fc (a–the relationship between PAR and Fc in the rainy season; b–the response of Fc to PAR during daytime in the rainy season).

3.4.2 Relationship with other environmental factors

With no significant correlation with SWC (Fig. 7a and 7b) shown by the daily scale NEE in the various seasons, there was a moderate negative correlation with Ta and Ts , and a strong positive correlation with RH and P. The daily scale NEE in the dry season has a moderate negative correlation with VPD, while the NEE in the rainy season shows a strong negative correlation with VPD. In general, due to the small variations in SWC within the two seasons (Fig. 2b), therefore, the impact of SWC on the diurnal fluctuation of the NEE was not significant. The diurnal variation of NEE in the dry season is mainly affected by RH and P, while the rainy season is mainly affected by RH and VPD, and the influence of other environmental factors is relatively weak.
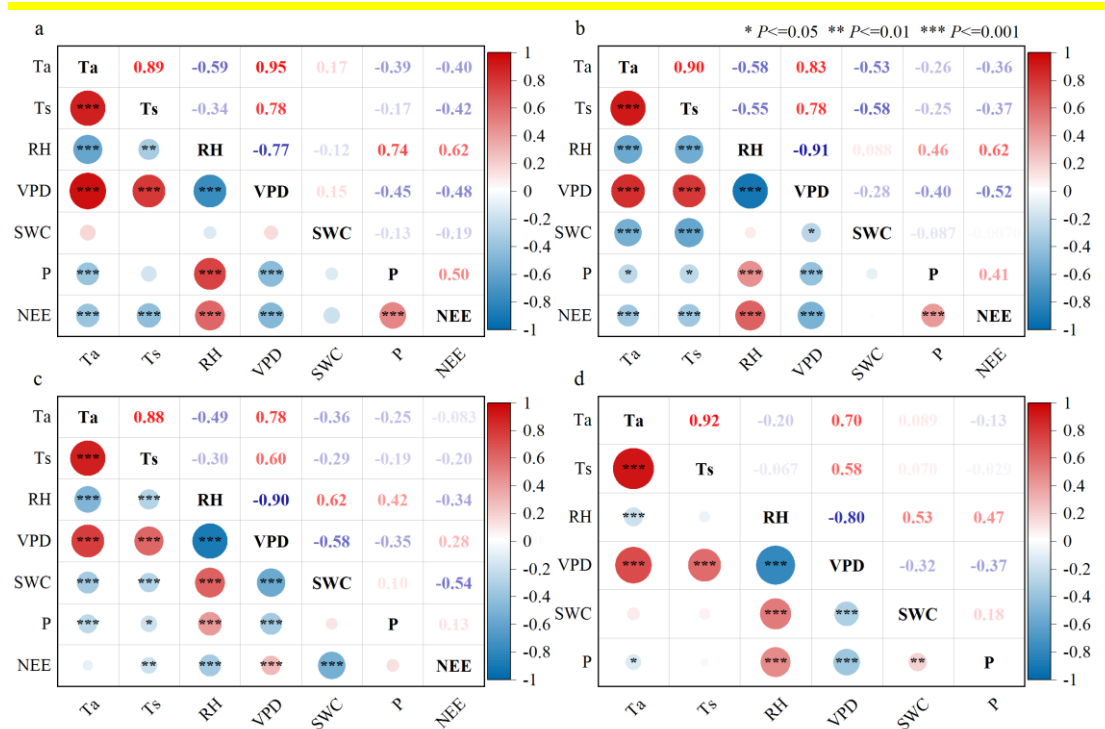
13

a

	Ta	Ts	RH	VPD	SWC	P	NEE
Ta	**Ta**	0.89	-0.59	0.95	0.17	-0.39	-0.40
Ts	***	**Ts**	-0.34	0.78		-0.17	-0.42
RH	***	**	**RH**	-0.77	-0.12	0.74	0.62
VPD	***	***	***	**VPD**	0.15	-0.45	-0.48
SWC					**SWC**	-0.13	-0.19
P	***		***	***		**P**	0.50
NEE	***	***	***	***		***	**NEE**

b *P<=0.05 ** P<=0.01 *** P<=0.001*

	Ta	Ts	RH	VPD	SWC	P	NEE
Ta	**Ta**	0.90	-0.58	0.83	-0.53	-0.26	-0.36
Ts	***	**Ts**	-0.55	0.78	-0.58	-0.25	-0.37
RH	***	***	**RH**	-0.91	0.088	0.46	0.62
VPD	***	***	***	**VPD**	-0.28	-0.40	-0.52
SWC	***	***		*	**SWC**	-0.087	0.087
P	*	*	***	***		**P**	0.41
NEE	***	***	***	***		***	**NEE**

c

	Ta	Ts	RH	VPD	SWC	P	NEE
Ta	**Ta**	0.88	-0.49	0.78	-0.36	-0.25	-0.083
Ts	***	**Ts**	-0.30	0.60	-0.29	-0.19	-0.20
RH	***	***	**RH**	-0.90	0.62	0.42	-0.34
VPD	***	***	***	**VPD**	-0.58	-0.35	0.28
SWC	***	***	***	***	**SWC**	0.10	-0.54
P	***	*	***	***		**P**	0.13
NEE		**	***	***	***		**NEE**

d

	Ta	Ts	RH	VPD	SWC	P
Ta	**Ta**	0.92	-0.20	0.70	0.089	-0.13
Ts	***	**Ts**	-0.067	0.58	0.070	-0.029
RH	***		**RH**	-0.80	0.53	0.47
VPD	***	***	***	**VPD**	-0.32	-0.37
SWC			***	***	**SWC**	0.18
P	*		***	***	**	**P**

Figure 7 The Pearson correlation between F*c* and environmental factors (a–daily scales of the dry season; b–daily scales of the rainy season; c–annual daily scales; d–the correlation between different environmental factors, the data is consistent with Fig. 2).

Throughout the year on a daily scale (Fig. 7c), the NEE showed no significant correlation with Ta and P, a weak positive correlation with VPD, a weak negative correlation with Ts, a moderate negative correlation with RH, and a strong negative correlation with SWC. It is evident that as the time series extends, the physiological responses of photosynthesis and respiration processes in the open savanna to specific environmental factors have changed. Particularly, the impact of SWC was most significant, closely related to the distinct climatic characteristics of wet and dry seasons in the study area. Under such climatic conditions, the variation in SWC throughout the year becomes the dominant factor restricting regional vegetation growth and recovery (Jiang et al., 2007), significantly influencing the intra-annual variation of the F*c*.

In terms of environmental factors(Fig. 7d), Ta shows a strong positive correlation with Ts and VPD, and a weak negative correlation with RH. P has a weak negative correlation with Ta, a moderate negative correlation with VPD, a weak positive correlation with SWC, and a moderate positive correlation with RH. SWC has a strong positive correlation with RH and a moderate negative correlation with VPD. The relationship between Ts and SWC with P is not significant, which should be related to the lag effect of P.

14

4 Discussion

4.1 CO_2 flux of the open savanna

The herbs in the study area are mainly C_4 plants (Grace et al., 1995), which are called high-efficiency photosynthetic plants, and the C_4 plants exhibit higher efficiency in photosynthesis and resource utilization when compared to C_3 plants (Cui et al., 2021; Arslan et al., 2023). However, the open savanna has been in a dry, high-temperature, and low-rainy climate for a long time. This extreme climatic condition makes the productivity of C_4 herbaceous plants only maintained at a medium level (Grace et al., 2006). The daily maximum CO_2 uptake rate was recorded at only 1.9585 $\mu mol \cdot m^{-2} \cdot s^{-1}$, which stands notably lower in comparison to other savanna ecosystems (10 to 15 $\mu mol \cdot m^{-2} \cdot s^{-1}$) and grasslands found in arid and semi-arid regions (2.16 to 7.90 $\mu mol \cdot m^{-2} \cdot s^{-1}$) (Grace et al., 2006; Du et al., 2012; Niu et al., 2018; Hu et al., 2018; Zhang et al., 2020; Guo et al., 2022). Furthermore, the most savanna ecosystems globally demonstrate C sequestration features, with only a few exhibiting characteristics of C emissions (Fei et al., 2017b). Among them, the savanna ecosystem with C source characteristics is mainly grassland savanna and semi-arid savanna, especially the grassland savanna has the largest annual C emissions (Archibald et al., 2009; Hutley et al., 2005; Quansah et al., 2015), which is similar to the results of this study. In the arid/semi-arid regions of China, the NEE of different grasslands varies between −3.08 to 0.96 t $C \cdot ha^{-1} \cdot a^{-1}$ (Du et al., 2012; Niu et al., 2018; Chen et al., 2019; Zhang et al., 2020; Bai et al., 2022). We also found that most grasslands act as C sinks, with only a few, such as the Horqin sandy grassland (Niu et al., 2018; Chen et al., 2019), exhibiting C source characteristics, and the C emissions (0.91 to 0.96 t $C \cdot ha^{-1} \cdot a^{-1}$) is higher than those of the open savanna in the study area. Overall, the open savanna within the study area predominantly exhibits C emission, but at a relatively low level, displaying a C-neutral trait.

Compared to other savanna ecosystems and the majority of grasslands in arid and semi-arid regions, the open savanna in the study area not only have a lower C absorption capacity but also exhibit a C emission characteristic. This is partly due to the study area's unique high-temperature and dry hot island climate characteristics, and partly because the southwestern region of China experienced a record-breaking extreme drought event in 2023 (Wang et al., 2025), which significantly reduced vegetation productivity and also led to the study area's rainfall reaching the lowest level in nearly four decades (Fig. 3). This further exacerbated the ecological drought of the open savanna, causing a substantial decrease in the C absorption capacity of the ecosystem and an increase in the total annual C emissions.

4.2 Effects of environmental factors on CO_2 flux

4.2.1 Temperature factor

The temperature affects the Fc of terrestrial ecosystems by regulating biological activities such as photosynthesis and respiration (Pan et al., 2020; Johnston et al., 2021; Chen et al., 2023), especially for grassland ecosystems, several studies have validated that temperature serves as the primary driving force controlling the variation in Fc. Nevertheless, owing to variations in environmental conditions, the regulatory impact of temperature fluctuations on the Fc differs significantly across various types of grassland ecosystems. Compared with temperate grasslands and semi-arid grasslands, the warming effect has the most significant impact on the Fc of frigid grasslands worldwide (Wang et al., 2019). The rise in temperature (both annual average temperature and annual average soil temperature) reduced the Fc of temperate grasslands in China, while the effect on alpine grasslands was the opposite (Liu et al., 2024). In the Inner Mongolia Plateau, with the increase of temperature, the NEE of the grassland will increase (Liu et al., 2018), whereas the change on the Qinghai-Tibet Plateau is much smaller in comparison. There is no correlation between Fc and temperature change in the Inner Mongolia grassland during the drought period (Hao et al., 2006). The Ta and Ts exhibit a negative correlation with the Fc at different seasonal daily scales in the open savanna in the dry-hot valley of JS (Fig. 7a and 7b). As the temporal scale increases, the impact of Ta and Ts on the fluctuations in the Fc continues to weaken(Fig. 7c), which is related to the small differences in Ta and Ts within different time scales in the study area. That is, the small temperature difference leads to the distribution change of the Fc in time is not sensitive to temperature fluctuation, which is similar to the impact mechanisms seen in other arid and semi-arid grasslands (Li et al., 2015; Niu et al., 2018; Chen et al., 2019; Wang et al., 2021).

To further explore the environmental drivers of Fc, we employed a quadratic regression model to quantitatively analyze and predict the response of NEE to Ta, Ts, RH, VPD, P, and SWC (Fig. 8, 9, and 10). From the regression results (Fig. 8a and 8b), it was observed that the NEE of the open savanna primarily decreases gradually with an increase in Ta. During the dry season, when the Ta exceeds 28.83°C, the C emissions from the ecosystem gradually increase. In the rainy season, when the Ta surpasses 25.50°C, the C sequestration capacity rapidly declines, which is roughly consistent with the temperature threshold (Ta=24.7°C) of the YJ savanna (Fei et al., 2017b). Similarly, a comparable change trend was observed between NEE and Ts (Fig. 8g and 8h), that is, when Ts exceeded 32.41°C and 29.81°C respectively, the C emissions increased during the dry season of the open savanna, and the C sequestration capacity decreased during the rainy season.
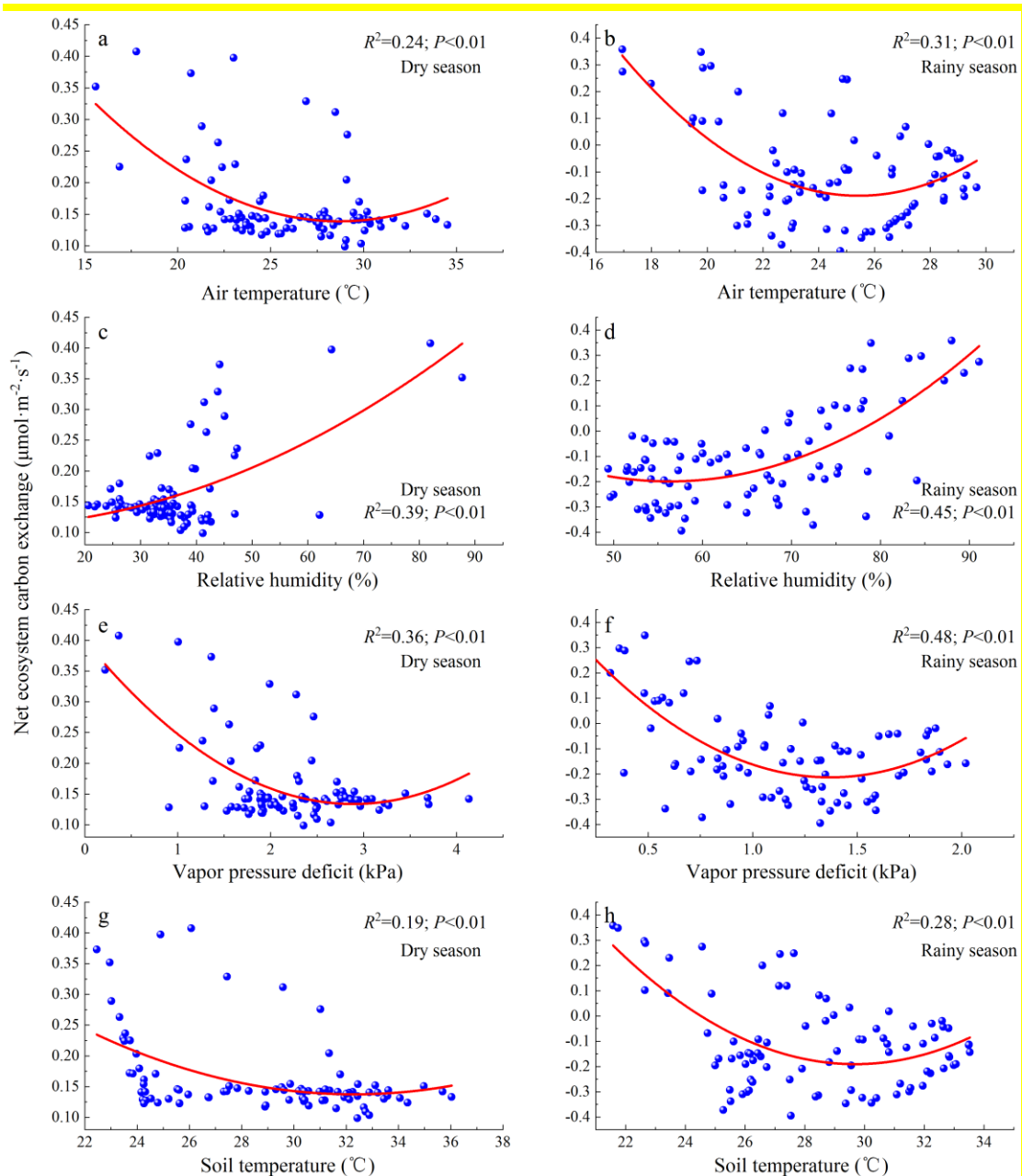
Figure 8 The response of Fc to environmental factors (a–the response of NEE to Ta in dry season; b–the response of NEE to Ta in rainy season; c–the response of NEE to RH in dry season; d–the response of NEE to RH in rainy season; e–the response of NEE to VPD in dry season; f–the response of NEE to VPD in rainy season; g–the response of NEE to Ts in dry season; h–the response of NEE to Ts in rainy season).

4.2.2 Water factor

A potential limiting factor affecting C uptake in terrestrial ecosystems is soil moisture, which can diminish net primary production through water stress in ecosystems, leading to vegetation death (Green et al., 2019). Simultaneously, soil moisture may exacerbate extreme climatic conditions through the intricate interaction between the land and the atmosphere. Particularly in arid regions, there exists a significant interaction between soil moisture and vegetation. Hence, in terms of Fc affecting dryland ecosystems, SWC is a more important control factor than Ta (Zou et al., 2016;

17

Tarin et al., 2020; Kannenberg et al., 2024). For instance, in the herbs growth season of the Qinghai–Tibet Plateau, regions with plentiful precipitation in the east and southeast primarily regulate C absorption capacity through temperature. Conversely, SWC emerges as the principal determinant of C sequestration capability in the arid and water shortage western region (Wang et al., 2021). Simultaneously, the SWC emerges also as the predominant factor influencing the diurnal fluctuations of NEE in grassland in the semi-arid regions of northern China (Zhao et al., 2020).

To further assess the impact of SWC on NEE, we divided the SWC into three levels: low SWC (0 $m^3 \cdot m^{-3} \leq$ SWC ≤ 0.05 $m^3 \cdot m^{-3}$), moderate SWC (0.05 $m^3 \cdot m^{-3} <$ SWC≤ 0.10 $m^3 \cdot m^{-3}$), and high SWC (0.10 $m^3 \cdot m^{-3} <$ SWC), corresponding to dry, intermediate, and wet periods, respectively. We then analyzed the relationship between SWC and NEE during these different periods (Fig. 9a). During the dry period, SWC showed a weak negative correlation with NEE. In the intermediate period, there was a strong negative correlation between SWC and NEE. In the wet period, SWC exhibited a strong positive correlation with NEE. In addition, we can also observe that the NEE of the open savanna in the study area exhibits a parabolic trend of first decreasing and then increasing with the increase in SWC (Fig. 9b). This indicates that the maximum value of NEE typically occurs at the two extreme SWC values, while the minimum value of NEE appears at the position of moderate SWC. That is, when the SWC is in the dry period and the transition period, the C uptake capacity generally enhances with the increase in SWC, reaching a maximum under optimal conditions (SWC=$0.07 m^3 \cdot m^{-3}$), and then decreases in the flooded environment. Globally, Peng et al. (2024) has also found that the total gross primary productivity (GPP) of ecosystems exhibits a hump-shaped response curve with increasing soil moisture, indicating the presence of an apparent optimal soil moisture level. This phenomenon is widespread, even in arid and water-scarce regions (Taylor et al ., 2017; Kannenberg et al., 2024).
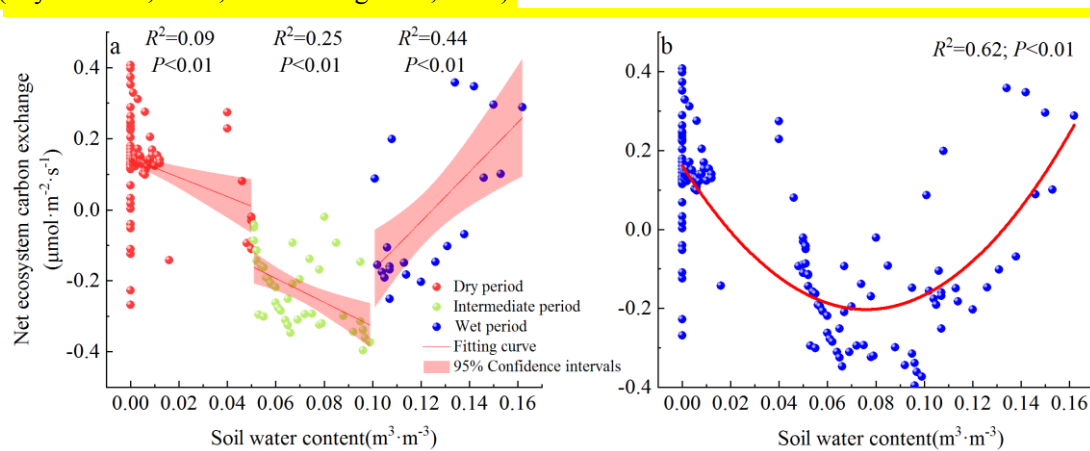

Figure 9 Effects of SWC on Fc (a–the relationship between NEE and SWC; b–the response of annual NEE to SWC).

It should be noted that the F_c and SWC in open savanna was influenced by multiple environmental factors. Therefore, when studying the response relationship between NEE and SWC, we analyzed the correlation coefficient between SWC and NEE under conditions where other environmental factors such as Ta, RH, and PAR were controlled or not. The results showed no significant difference ($R_{controlled} = -0.546$, $P<0.01$; $R = -0.535$, $P<0.01$), indicating that other environmental factors have no significant impact on the nonlinear relationship between NEE and SWC. In summary, for arid regions, both excessively low and high SWC can affect the C absorption capacity of ecosystems.

In arid ecosystem, the effectiveness of water dictates plant growth and the release and absorption of CO_2. Therefore, the F_c of grasslands in arid regions exhibits greater sensitivity to variations in the P (Knapp et al., 2002; Niu et al., 2007; Weltzin et al., 2003; Zhang et al., 2020). An increase in the P led to a delay in the peak of gross primary productivity in vegetation growth stage of the Inner Mongolia desert steppe, enhancing the ecosystem's F_c (Li et al., 2017; Zhang et al., 2019). The P of Xilinhot grassland changed the F_c in the vegetation growth season mainly by affecting SWC (Wang et al., 2015). High water levels (annual average precipitation and soil moisture) have continuously increased the F_c of temperate grasslands and alpine grasslands in the Mongolian Plateau, Loess Plateau, and Qinghai–Tibet Plateau (Liu et al., 2024). As far as the open savanna in the dry-hot valley of JS is concerned, the P shows a positive correlation with the F_c at different seasonal daily scales, with no significant relationship observed with the F_c variation on the daily scales throughout the year (Fig. 7a, 7b, and 10a). However, the variation in P significantly affects the regional SWC and RH (Fig. 7d). Therefore, the impact mechanism of the P on the F_c in the JS dry-hot valley open savanna may be similar to that of the Xilinhot grassland, where the P mainly controls vegetation growth by affecting SWC and RH, thereby indirectly influencing the F_c.

4.2.3 Relative humidity and vapor pressure deficit factor

As an important measure of atmospheric dryness, the fluctuation of VPD is controlled by RH and has a high correlation with other important driving factors of ecosystem productivity, such as Ta and SWC. Multiple studies have shown that when RH decreases, vegetation stomata will be closed due to an increase in VPD, thereby preventing excessive water loss (Williams et al., 2013; Novick et al., 2016; Sulman et al., 2016; Hsu et al., 2021), leading to a decrease in the photosynthetic rate of leaves and canopies, thereby inhibiting photosynthesis (McDowell et al., 2015; Sulman et al., 2016; Yuan et al., 2019). Therefore, there is a negative correlation between the intensity of plant photosynthesis and VPD. Globally, studies have also shown that increased VPD reduces vegetation growth and offsets the beneficial impacts of CO_2 fertilization (Yuan et al., 2019). Simultaneously,

the interannual variation of VPD shows a significant negative correlation with net ecosystem productivity and affects the interannual variation of atmospheric CO_2 growth rate (He et al., 2022). However, because of variations in climatic conditions and the synergistic effects of multiple environmental factors, the response mechanisms of the F_c in different grassland ecosystems to changes in VPD and RH are varied. For instance, in the savanna of YJ, the F_c shows a negative correlation with VPD (Fei et al., 2017a). Wang et al. (2021) found through a study on the spatial variation of F_c of 10 distinct grassland types that a positive correlation exists between VPD and NEE in the Qinghai–Tibet Plateau. In the arid grasslands of the Heihe River Basin (Bai et al., 2022), the F_c is also positively correlated with VPD and RH.
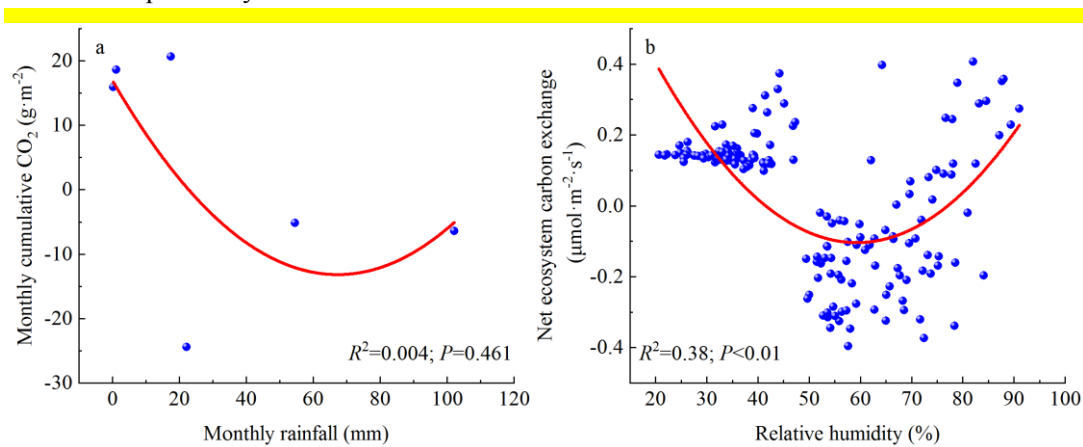

Figure 10 The response of F_c to monthly rainfall and annual RH (a–the response of monthly cumulative CO_2 to monthly rainfall; b–the response of annual NEE to RH).

In the study area, the daily-scale NEE and RH showed a positive correlation during different seasons, whereas a negative correlation was observed at interannual scales. This indicates that, over long-term time scales, an increase in RH enhances the C sequestration capacity of open savanna. The relationship between VPD and NEE was the opposite (Fig. 7a, 7b, and 7c). However, further regression analysis (Fig. 8c and 8d) revealed that during the rainy season, NEE initially decreases and then increases with rising RH, reaching a minimum value under certain conditions (RH=56.41%). This response was more clearly observed in the interannual quadratic regression model of NEE versus RH (Fig. 10b). A similar relationship was also found between NEE and VPD (Fig. 8e and 8f), with NEE rapidly increasing when VPD exceeds the thresholds of 2.89 kPa (dry season) and 1.37 kPa (rainy season), respectively, in different seasons, which is consistent with the control mechanism of the YJ savanna. (Fei et al., 2017b).

Overall, aside from the P factor, the maximum value of NEE in the open savanna of the JS dry-hot valley generally occurs at the two extreme values of various environmental factors, while the minimum value of NEE appears at positions of environmental factor threshold. However, as can be

observed from Fig. 7, the P is closely related to other environmental factors, with the continuous decrease in rainfall and the increasing severity of drought, Ta, Ts, and VPD will continuously rise, while SWC and RH will gradually decrease. That is, from the perspective of NEE's response to different environmental factors, as global warming continues to lead to a decrease in rainfall in the future, the C emissions from the open savanna in the study area will continue to rise. In addition, the study area experiences long-term drought, high temperatures, and low rainfall. Herbage vegetation has shown a stronger ability to adapt to ecological drought stress compared to other regions. However, the research has found that under the extreme drought event of 2023, the C sequestration capacity of the open savanna has still been significantly weakened. Secondly, the study area belongs to a special heat island habitat within the temperate climate zone, with climate characteristics and vegetation community structures representing the future scenarios of temperate ecosystems under conditions of continuous warming and decreasing precipitation. Particularly in recent years, there has been a shift of vegetation communities in some temperate regions towards savannas (Yang and Chang, 2007; Jing et al., 2024). As the frequency and severity of global droughts continue to rise, researchers have found that the sensitivity of vegetation in grasslands and arid regions to drought is significantly increasing, and the response time of vegetation productivity to drought is also gradually decreasing (Tang et al., 2024). Therefore, under climate scenarios where the frequency, duration, and severity of droughts are all on the rise, some grasslands in temperate climate regions may shift from being C sinks to carbon sources. This transition is of great importance for the C balance of global terrestrial ecosystems. Our research findings will provide important references for accurately predicting the C budget of terrestrial ecosystems under future extreme climatic conditions.

5 Conclusions

This study quantitatively analyzed the F_c variations and their relationships with environmental factors in the open savanna of the dry-hot valley of JS, further deepening the researchers' theoretical understanding of the changes in grassland C sequestration functions under extreme dry and hot climate conditions, and providing an effective reference for the accurate prediction of future terrestrial ecosystem C sink capacity. Nonetheless, the lack of long-term observational data on F_c in our study precludes a more thorough examination of the inter-annual variation characteristics of the F_c. Secondly, the study did not effectively monitor the dynamic characteristics of soil respiration, which made it impossible to accurately calculate the ecosystem's GPP. Furthermore, we only observed and studied the changes in F_c of the dominant grassy layer, while the dry-hot valley

ecosystem has a vegetation community structure with two levels of shrub and grass. Therefore, our forthcoming research will emphasize the extended observation of the Fc changes in the savanna ecosystem with a complete vegetation community structure, especially the use of eddy covariance methods to expand the scope of ecosystem observation and reduce the uncertainty of measurement samples, so as to better elucidate the carbon budget patterns of ecosystems under extreme climatic conditions. Through this research, we have arrived at the following findings:

(1) As a result of environmental factors, the Fc of the open savanna in the JS dry-hot valley exhibited significant temporal variations. During the dry season, the open savanna functioned as a C source, with the daily variation of Fc showing a 'W'-shaped bimodal curve. In contrast, during the rainy season, the open savanna functioned as a C sinks, with the daily variation of Fc displaying a 'U'-shaped unimodal curve. Overall, open savanna was a weak C source, exhibiting a C-neutral characteristic.

(2) During the dry season, the NEE of open savanna was primarily influenced by RH and P, whereas during the rainy season, NEE was mainly affected by PAR, VPD and RH. On a daily scale throughout the year, SWC had the most pronounced impact on NEE, while the influence of temperature factors on NEE was relatively minor. P primarily influences other environmental factors, thereby indirectly controlling changes in NEE.

(3) The response mechanism of NEE to changes in various environmental factors in open savannas was similar. Specifically, the maximum value of NEE generally occurred at the two extreme values of the various environmental factors, and NEE increased when either above or below the thresholds of environmental factors. This mechanism was most pronounced in the relationship between NEE and SWC.

(4) The occurrence of extreme drought events has weakened the carbon sequestration capacity of the open savannas in the study area. With the continued warming of the global climate leading to changes in future rainfall patterns and a decrease in rainfall, the carbon emissions from the open savannas are expected to continue to increase.

Data availability

References

Archibald, S.A., Kirton, A., van der Merwe, M.R., Scholes, R.J., Williams, C.A., Hanan, N.: Drivers of inter-annual variability in net ecosystem exchange in a semi-arid savanna ecosystem, South Africa, Biogeosci, 6, 251–266, 2009.

Ago, E.E., Agbossou, E.K., Galle, S., Cohard, J.M., Heinesch, B., Aubinet, M.: Long term observations of carbon dioxide exchange over cultivated savanna under a Sudanian climate in Benin (West Africa), Agric. For. Meteorol, 197, 13–25, https://doi.org/10.1016/j.agrformet.2014.06.005, 2014.

Arslan, A.M., Wang, X., Liu, B.Y., Xu, Y.N., Li, L., Gong, X.Y.: Photosynthetic resource-use efficiency trade-offs triggered by vapour pressure deficit and nitrogen supply in a C_4 species, Plant Physiol. Biochem, 197, 107666, https://doi.org/10.1016/j.plaphy.2023.107666, 2023.

Beringer, J., Hutley, L.B., Tapper, N.J., Cernusak, L.A.: Savanna fires and their impact on net ecosystem productivity in North Australia, Global Change Biol, 13, 990–1004, https://doi.org/10.1111/j.1365-2486.2007.01334.x, 2007.

Brümmer, C., Falk, U., Papen, H., Szarzynski, J., Wassmann, R., Brüggemann, N.: Diurnal, seasonal, and interannual variation in carbon dioxide and energy exchange in shrub savanna in Burkina Faso (West Africa), J. Geophys. Res.: Biogeosci, 113, https://doi.org/Artn G0203010.1029/2007jg000583, 2008.

Bai, X.J., Wang, X.F., Liu, X.H., Zhou, X.Q.: Dynamics and driving factors of carbon fluxes in wetland，cropland and grassland ecosystems in Heihe river basin, Remote Sens, Technol. Appl, 37, 94−107, https://doi.org/10.11873/j.issn.1004-0323.2022.1.0094, 2022.

Bai, X.Y., Zhang, S.R., Li, C.J., Xiong, L., Song, F.J., Du, C.C., Li, M.H., Luo, Q., Xue, Y.Y., Wang, S.J.: A carbon-neutrality-capacity index for evaluating carbon sink contributions, Environ. Sci. Ecotechnol., 15, 100237, https://doi.org/10.1016/j.ese.2023.100237, 2023.

Bureau of Statistics of Yunnan Province. Yunnan Statistical Yearbook; China Statistics Press: Beijing, China, 2023.

Campbell, G.S., Norman, J.M.: An introduction to environmental biophysics, Springer Sci, Business Media, 2012.

Cleverly, J. Boulain, N., Villalobos-Vega, R., Grant, N., Faux, R., Wood, C., Cook, P.G., Yu, Q., Leigh, A., Eamus, D.: Dynamics of component carbon fluxes in a semi-arid Acacia woodland, central Australia, J. Geophys. Res.: Biogeosci, 118, 1168–1185, https://doi.org/10.1002/jgrg.20101, 2013.

Carey, C.J., Tang, J.W., Templer, P.H., Kroeger, K.D., Crowther, T.W., Burton, A.J., Dukes, J.S., Emmett, B., Frey, S.D., Heskel, M.A., Jiang, L.F., Machmuller, M.B., Mohan, J., Panetta, A.M., Reich, P.B., Reinsch, S., Wang, X., Allison, S.D., Bamminger, C., Bridgham, S., Collins, S.L., de Dato, G., Eddy, W.C., Enquist, B.J., Estiarte, M., Harte, J., Henderson, A., Johnson, B.R., Larsen, K.S., Luo, Y.Q., Marhan, S., Melillo, J.M., Peñuelas, J., Pfeifer-Meister, L., Poll, C., Rastetter, E., Reinmann, A.B., Reynolds, L.L., Schmidt, I.K., Shaver, G.R., Strong, A.L., Suseela, V., Tietema, A.: Temperature response of soil respiration largely unaltered with experimental warming, PNAS, 113, 13797−13802, https://doi.org/10.1073/pnas.1605365113, 2016.

Chen, Y.P., Niu, Y.Y., Li, W., Li, Y.Q., Gong, X.W., Wang, X.Y.: Characteristics of carbon flux in sandy grassland ecosystem under natural restoration in Horqin sandy land, Plateau Meteorol, 38, 650–659, https://doi.org/10.7522/.issn.1000-0534.2018.00133, 2019.

Cui, H.C.: Challenges and approaches to crop improvement through C_3-to-C_4 engineering, Front. Plant Sci, 12, 715391, https://doi.org/10.3389/fpls.2021.715391, 2012.

Chen, W.N., Wang, S., Wang, J.S., Xia, J.Y., Luo, Y.Q., Yu, G.R., Niu, S.L.: Evidence for widespread thermal optimality of ecosystem respiration, Nat. Ecol. Evol, 7, 1379–1387, https://doi.org/10.1038/s41559-023-02121-w, 2023.

Du, Q., Liu, H.Z., Feng, J.W., Wang, L., Huang, J.P., Zhang, W., Bernhofer, C.: Carbon dioxide exchange processes over the grassland ecosystems in semiarid areas of China, Sci. China, Ser. D Earth Sci, 42, 711–722, https://doi.org/10.1007/s11430-011-4283-1, 2012.

Dobson, A., Hopcraft, G., Mduma, S., Ogutu, J.O., Fryxell, J., Anderson, M., Archibald, S., Lehmann, C., Poole, J., Caro, T., Mulder, M.B., Holt, R.D., Berger, J., Rubenstein, D.I., Kahumbu, P., Chidumayo, E.N., Milner-Gulland, E.J., Schluter, D., Otto, S., Balmford, A., Wilcove, D., Pimm, S., Veldman, J.W., Olff, H., Noss, R., Holdo, R., Beale, C., Hempson, G., Kiwango, Y., Lindenmayer, D., Bond, W., Ritchie M., Sinclair, A.R.E.: Savannas are vital but overlooked carbon sinks, Science, 375, 392, https://doi.org/10.1126/science.abn4482, 2022.

Deng, Y.: The boundary definition and studyon the land use/cover change and landscape pattern of the dry-hot valley in Hengduan Mountains, Yunnan University, https://doi.org/10.27456/d.cnki.gyndu.2022.000408, 2022.

Eamus, D., Hutley, L.B., O'Grady, A.P.: Daily and seasonal patterns of carbon and water fluxes above a north Australian savanna, Tree Physiol, 21, 977–988, 2001.

Fei, X.H., Song, Q.H., Zhang, Y.P., Liu, Y.T., Sha, L.Q., Yu, G.R., Zhang, L.M., Duan, C.Q., Deng, Y., Wu, C.S., Lu, Z.Y., Luo, K., Chen, A.G., Xu, K., Liu, W.W., Huang, H., Jin, Y.Q., Zhou, R.W., Li, J., Lin, Y.X., Zhou, L.G., Fu, Y., Bai, X.L., Tang, X.H., Gao, J.B., Zhou, W.J., Grace, J.: Carbon exchanges and their responses to temperature and precipitation in forest ecosystems in Yunnan, Southwest China, Sci. Total Environ, 616–617, 824–840, https://doi.org/10.1016/j.scitotenv.2017.10.239, 2017a.

Fei, X.H., Jin, Y.Q., Zhang, Y.P., Sha, L.Q., Liu, Y.T., Song, Q.H., Zhou, W.J., Liang, N.S., Yu, G.R.,

Zhang, L.M., Zhou, R.W., Li, J., Zhang, S.B., Li, P.G.: Eddy covariance and biometric measurements show that a savanna ecosystem in Southwest China is a carbon sink, Sci Rep, 7, 41025, https://doi.org/10.1038/srep41025, 2017b.

Grace, J., Lloyd, J., McIntyre, J., Miranda, A.C., Meir, P., Miranda, H., Moncrieff, J.M., Massheder, J., Wright, I.R., Gash, J.: Fluxes of carbon dioxide and water vapour over an undisturbed tropical forest in south-west Amazonia, Global Change Biol, 1, 1–12, https://doi.org/10.1111/j.1365-2486.1995.tb00001.x, 1995.

Grace, J., José, J. S., Meir, P., Miranda, H. S., Montes, R.A.: Productivity and carbon fluxes of tropical savannas, J. Biogeogr, 33, 387–400, https://doi.org/10.1111/j.1365-2699.2005.01448.x., 2006.

Green, J. K., Seneviratne, S. I., Berg, A. M., Findell, K. L., Hagemann, S., Lawrence, D. M., Gentine, P.: Large influence of soil moisture on long-term terrestrial carbon uptake, Nature, 565, 476–479, https://doi:10.1038/s41586-018-0848-x, 2019.

Guo, W.Z., Jing, C.Q., Deng, X.J., Chen, C., Zhao, W.K., Hou, Z.X., Wang, G.X.: Variations in carbon flux and factors influencing it on the northern slopes of the Tianshan Mountains, Acta Prataculturae Sin, 31, 1−12. https://doi.org/10.11686/cyxb2021137, 2022.

He, Y.B., Lu, P.Z., Zhu, T.: Causes for the formation of dry-hot valleys in Hengduan Mountain-Yunnan plateau, Resour. Sci, 22, 69–72, https://www.resci.cn/CN/Y2000/V22/I5/69, 2000.

Hutley, L.B., Leuning, R., Beringer, J., Cleugh, H.A.: The utility of the eddy covariance techniques as a tool in carbon accounting: tropical savanna as a case study, Aust. J. Bot, 53, 663–675, https://doi.org/10.1071/Bt04147, 2005.

Hao, Y.B., Wang, Y.F., Sun, X.M., Huang, X.Z., Cui, X.Y., Niu, H.S., Zhang, Y.H., Yu, G.R.: Seasonal variation in carbon exchange and its ecological analysis over Leymus chinensis steppe in Inner Mongolia, Sci. China, Ser. D Earth Sci, 49, 186–195, https://doi.org/10.1007/s11430-006-8186-5, 2006.

Harmon, T.C., Dierick, D., Trahan, N., Allen, M.F., Rundel, P.W., Oberbauer, S.F., Schwendenmann, L., Zelikova, T.J.: Low−cost soil CO_2 efflux and point concentration sensing systems for terrestrial ecology applications, Methods Ecol. Evol, 6, 1358–1362, https://doi.org/10.1111/2041-210X.12426, 2015.

Hu, Y., Zhu, X.P., Jia, H.T., Han, D.L., Hu, B.A., Li, D.P.: Effects of fencing on ecosystem crabon exchange at meadow steppe in the northern slop oh the Tianshan Mountains, Chinese J. Plant Eco, 42, 372–381, https://doi.org/10.17521/cjpe.2016.0049, 2018.

Hsu, P.K., Takahashi, Y., Merilo, E., Costa, A., Zhang, L., Kernig, K., Lee, K.H., Schroeder, J.I.: Raf-like kinases and receptor-like (pseudo)kinase GHR1 are required for stomatal vapor pressure difference response, PNAS, 118, e2107280118, https://doi.org/10.1073/pnas.21072801, 2021.

He, B., Chen, C., Lin, S.R., Yuan, W.P., Chen, H.W., Chen, D.L., Zhang, Y.F., Guo, L.L., Zhao, X., Liu, X.B., Piao, S.L., Zhong, Z.Q., Wang, R., Tang, R.: Worldwide impacts of atmospheric vapor pressure deficit on the interannual variability of terrestrial carbon sinks, Natl. Sci. Rev, 9, nwab150, https://doi.org/10.1093/nsr/nwab150, 2022.

Hoffmann, W.A.: Seasonal flooding shapes forest–savanna transitions, PNAS, 120, e2312279120, https://doi.org/10.1073/pnas.2312279120, 2023.

He, G.X., Shi, Z.T., Fang, H.D., Shi, L.T., Wang, Y.D., Yang, H.Z., Yan, B.G., Yang, C.L., Yu, J.L., Liang, Q.L., Zhao, L., Jiang, Q.: Climate and soil stressed elevation patterns of plant species to

determine the aboveground biomass distributions in a valley-type Savanna, Front. Plant Sci, 15, 1324841, https://doi.org/10.3389/fpls.2024.1324841, 2024.

Huang, M.T., Zhai, P.M.: Impact of extreme seasonal drought on ecosystem carbon–water coupling across China, Adv. Clim. Change Res, 15, 914−923, https://doi.org/10.1016/j.accre.2024.08.001, 2024.

IPCC (Intergovernmental Panel on Climate Change).: Climate Change 2021: the Physical Science Basis. Contribution of Working Group I to the Sixth Assessment Report of the Intergovernmental Panel on Climate Change, Cambridge University Press, Cambridge, UK, 2021.

Jin, Z.Z., Ou, X.K., Zhou, Y.: The general situation of natural vegetation in dry-hot river valley of Yuanmou, Yunnan Province, Chin. J. Plant Ecol, 11, 308−317, 1987.

Jiang, J.M., Fei, S.M., He, Y.P., Zhang, F., Kong, Q.H.: Study on vegetation restoration in dry-hot valleys of the Jinsha River, J. Southwest For. Univ, 27, 11–15, https://doi.org/10.11929/j.issn.2095-1914.2007.06.003, 2007.

Jin, Y.Q., Li, J., Liu, C.G., Liu, Y.T., Zhang, Y.P., Song, Q.H., Sha, L.Q., Balasubramanian, D., Chen, A.G., Yang, D.X., Li, P.G.: Precipitation reduction alters herbaceous community structure and composition in a savanna, J. Veg. Sci, 30, 821–831, https://doi.org/10.1111/jvs.12766, 2019.

Johnston, A.S.A., Meade, A., Ardö, J., Arriga, N., Black, A., Blanken, P.D., Bonalo, D., Brümmer, C., Cescatti, A., Duševšeko, J., Grafo, A., Gioli, B., Godedo, I., Gougho, C.M., Ikawa, H., Jassalo, R., Kobayashi, H., Magliulo, V., Mancao, G., Montagnani, L., Moyano, F.E., Olesen, J.E., Sachs, T., Shao, C.L., Tagesson, T., Wohlfahrt, G., Wolfo, S., Woodgate, W., Varlagin, A., Venditti, C.: Temperature thresholds of ecosystem respiration at a global scale, Nat. Ecol. Evol, 5, 487–494, https://doi.org/10.1038/s41559-021-01398-z, 2021.

Jiang, Q.Q., He, J.J., Li, Y.R., Yang, X.Y., Peng, Y., Wang, H., Yu, F., Wu, J., Gong, S.L., Che, H.Z., Zhang, X.Y.: Analysis of the spatiotemporal changes in global land cover from 2001 to 2020, Sci. Total Environ., 908, 168354, https://doi.org/10.1016/j.scitotenv.2023.168354, 2024.

Knapp, A., Fay, P.A., Blair, J.M., Collins, S., Smith, M.D., Carlisle, J.D., Harpper, C.W., Danner, B.T., Lett, M.S., Mccarron, J.: Rainfall variability, carbon cycling, and plant species diversity in a mesic grassland, Science, 298, 2202−2205, https://doi.org/10.1126/science.1076347, 2002.

Kato, T., Tang, Y.H., Gu, S., Hirota, M., Du, M.Y., Li, Y.N., Zhao, X.Q.: Temperature and biomass influences on interannual changes in CO_2 exchange in an alpine meadow on the Qinghai-Tibetan Plateau, Global Change Biol, 12, 1285−1298, https://doi.org/10.1111/j.1365-2486.2006.01153.x, 2006.

Kannenberg, S.A., Anderegg, W.R.L., Barnes, M.L., Dannenberg, M.P., Knapp, A.K.: Dominant role of soil moisture in mediating carbon and water fluxes in dryland ecosystems, Nat. Geosci, 17, 38–43, https://doi.org/10.1038/s41561-023-01351-8, 2024.

Law, B.E., Falge, E., Gu, L., Baldocchi, D.D., Bakwin, P., Berbigier, P., Davis, K., Dolman, A.J., Falk, M., Fuentes, J.D., Goldstein, A., Granier, A., Grelle, A., Hollinger, D., Janssens, I.A., Jarvis, P., Jensen, N.O., Katul, G., Mahli, K., Matteucci, G., Meyers, T., Monson, R., Munger, W., Oechel, W., Olson, R., Pilegaard, K., Paw U, K. T., Thorgeirsson, H., Valentini, R., Verma, Shashi., Vesala, T., Wilson, K., Wofsy, S.: Environmental controls over carbon dioxide and water vapor exchange of terrestrial vegetation, Agric. For. Meteorol, 113, 97–120, https://doi.org/10.1016/S0168-1923(02)00104-1, 2002.

Li, S.G., Asanuma, J., Eugster, W., Kotani, A., Liu, J.J., Urano, T., Oikawa, T., Davaa, G.,

Oyunbaatar, D., Sugita, M.: Net ecosystem carbon dioxide exchange over grazed steppe in central Mongolia, Global Change Biol, 11, 1941–1955, https://doi.org/10.1111/j.1365-2486.2005.01047.x, 2005.

Livesley, S. J., Grover, S., Hutley, L.B., Jamali, H., Butterbach-Bahl, K., Fest, B., Arndt, S. K.: Seasonal variation and fire effects on CH_4, N_2O and CO_2 exchange in savanna soils of northern Australia, Agric. For. Meteorol, 151, 1440–1452, https://doi.org/10.1016/j.agrformet.2011.02.001, 2011.

Li, J.X., Zeng, H., Zhu, J.T., Zhang, Y.J., Chen, N., Liu, Y.J.: Responses of different experimental warming on ecosystem respiration in Tibetan alpine meadow, Ecol. Environ. Sci, 25, 1612–1620, https://doi.org/10.16258/j.cnki.1674-5906.2016.10.004, 2016.

Li, G.Y., Han, H.Y., Du, Y., Hui, D.F., Xia, J.Y., Niu, S.L., Li, X.N., Wan, S.Q.: Effects of warming and increased precipitation on net ecosystem productivity: a long-term manipulative experiment in a semiarid grassland, Agric. For. Meteorol, 232, 359−366, http://dx.doi.org/10.1016/j.agrformet.2016.09.004, 2017.

Liu, D., Li, Y., Wang, T., Peylin, P., MacBean, N., Ciais, P., Jia, G., Ma, M.G., Ma, Y.M., Shen, M.G., Zhang, X.Z., Piao, S.L.: Contrasting responses of grassland water and carbon exchanges to climate change between Tibetan Plateau and InnerMongolia, Agric. For. Meteorol, 249, 163–175, https://doi.org/10.1016/j.agrformet. 2017.11.034, 2018.

Lee, E., Kumar, P., Barron-Gafford, G.A., Hendryx, S.M., Sanchez-Cañete, E.P., Minor, R.L., Colella, T., Scott, R.L.: Impact of hydraulic redistribution on multispecies vegetation water use in a semiarid savanna ecosystem: an experimental and modeling synthesis, Water Resour. Res, 54, 4009–4027, https://doi.org/10.1029/2017WR021006, 2018.

Liu, J.X., Wang, Z., Duan, Y.F., Li, X.R., Zhang, M.Y., Liu, H.Y., Xue, P., Gong, H.B., Wang, X., Chen, Y., Geng, Y.N.: Effects of land use patterns on the interannual variations of carbon sinks of terrestrial ecosystems in China, Ecol. Indic, 146, 109914, https://doi.org/10.1016/j.ecolind.2023.109914, 2023.

Liu, Z.G., Chen, Z., Yang, M., Hao, T.X., Yu, G.R., Zhu, X.J., Zhang, W.K., Ma, L.X., Dou, X.J., Lin, Y., Luo, W.X., Han, L., Sun, M.Y., Chen, S.P., Dong, G., Gao, Y.H., Hao, Y.B., Jiang, S.C., Li, Y.N., Li, Y.Z., Liu, S.M., Shi, P.L., Tang, Y.K., Xin, X.P., Zhang, F.W., Zhang, Y.J., Zhao, L., Zhou, L., Zhu, Z.L.: Precipitation consistently promotes, but temperature oppositely drives carbon fluxes in temperate and alpine grasslands in China, Agric. For. Meteorol, 344, 109811, https://doi.org/10.1016/j.agrformet.2023.109811, 2024.

Miranda, A.C., Miranda, H.S., Lloyd, J., Grace, J., Francey, R.J., McIntyre, J.A., Meir, P., Riggan, P., Lockwood, R., Brass, J.: Fluxes of carbon, water and energy over Brazilian cerrado, an analysis using eddy covariance and stable isotopes, Plant Cell Environ, 20, 315–328, https://doi.org/10.1046/j.1365-3040.1997.d01-80.x, 1997.

Ma, S.Y., Baldocchi, D.D., Xu, L.K., Hehn, T.: Inter-annual variability in carbon dioxide exchange of an oak/grass savanna and open grassland in California, Agric. For. Meteorol, 147, 157–171. https://doi.org/10.1016/j.agrformet.2007.07.008, 2007.

Millard, P., Midwood, A. J., Hunt, J.E., Whitehead, D., Boutton, T.W.: Partitioning soil surface CO_2 efflux into autotrophic and heterotrophic components, using natural gradients in soil $\delta^{13}C$ in an undisturbed savannah soil, Soil Biol. Biochem, 40, 1575−1582, https://doi.org/10.1016/j.soilbio.2008.01.011, 2008.

McDowell, N.G., Allen, C.D.: Darcy's law predicts widespread forest mortality under climate

792 warming, Nat. Clim. Change, 5, 669–72, https://doi.org/10.1038/nclimate2641, 2015.

793 Niu, S.L., Wu, M.Y., Han, Y., Xia, J.Y., Li, L.H., Wan, S.Q.: Water-mediated responses of ecosystem
794 carbon fluxes to climatic change in a temperate steppe, New Phytol, 177, 209−219,
795 https://doi.org/10.1111/j.1469-8137. 2007.02237.x, 2017.

796 Novick, K.A., Miniat, C.F., Vose, J.M.: Drought limitations to leaf-level gas exchange: results from
797 a model linking stomatal optimization and cohesion–tension theory, Plant Cell Environ, 39, 583–
798 96, https://doi.org/10.1111/pce.12657, 2016.

799 Niu, Y.Y., Li, Y.Q., Wang, X.Y., Gong, X.W., Luo, Y.Q., Tian, D.Y.: Characteristics of annual
800 variation in net carbon dioxide flux in a sandy grassland ecosystem during dry years, Acta
801 Prataculturae Sin, 27, 215–221, https://doi.org/10.11686/cyxb2017231, 2018.

802 Peel, M.C., Finlayson, B.L., McMahon, T.A.: Updated world map of the Köppen-Geiger climate
803 classification, Hydrol. Earth Syst, Sci. 11, 1633–1644, https://doi.org/10.5194/hess-11-1633-
804 2007, 2007.

805 Piao, S.L., Huang, M.T., Liu, Z., Wang, X.H., Ciais, P., Canadell, J.G., Wang, K., Bastos, A.,
806 Friedlingstei, P., Houghto, R.A., Quéré, C.L., Liu, Y.W., Myneni, R.B., Peng, S.S., Pongratz, J.,
807 Sitch, S., Yan, T., Wang, Y.L., Zhu, Z.C., Wu, D.H., Wang, T.: Lower land-use emissions
808 responsible for increased net land carbon sink during the slow warming period, Nat. Geosci. 11,
809 739–743, https://doi.org/10.1038/s41561-018-0204-7, 2018.

810 Pan, S.F., Yang, J., Tian, H.Q., Shi, H., Chang, J.F., Ciais, P., Francois, L., Frieler, K., Fu, B.J.,
811 Hickler, T., Ito, A., Nishina, K., Ostberg, S., Reyer, C.P.O., Schaphoff, S., Steinkamp, J., Zhao,
812 F.: Climate extreme versus carbon extreme: responses of terrestrial carbon fluxes to temperature
813 and precipitation, J. Geophys. Res.: Biogeosci, 125, e2019JG005252,
814 https://doi.org/10.1029/2019JG005252, 2020.

815 ==Peng, J.L., Tang, J.W., Xie, S.D., Wang, Y.H., Liao, J.Q., Chen, C., Sun, C.L., Mao, J.H., Zhou, Q.P.,==
816 ==Niu, S.L.: Evidence for the acclimation of ecosystem photosynthesis to soil moisture, Nat.==
817 ==Commun., 15, 9795, https://doi.org/10.1038/s41467-024-54156-7, 2024.==

818 Quansah, E., Mauder, M., Balogun, A.A., Amekudz, L.K., Hingerl, L., Bliefernicht, J., Kunstmann,
819 H.: Carbon dioxide fluxes from contrasting ecosystems in the Sudanian savanna in West Africa,
820 Carbon Balance Manage, 10, 1, https://doi.org/10.1186/s13021-014-0011-4, 2015.

821 Ruimy, A., Jarvis, P.G., Baldocchi, D.D., Saugier, B.: CO_2 fluxes over plant canopies and solar
822 radiation: a review, Adv. Ecol. Res, 26, 1–68, https://doi.org/10.1016/s0065-2504(08)60063-x,
823 1995.

824 Santos, A.J.B., Silva, G.T.D.A., Miranda, H.S., Miranda, A.C., Lloyd, J.: Effects of fire on surface
825 carbon, energy and water vapour fluxes over campo sujo savanna in central Brazil, Funct. Ecol,
826 17, 711–719, https://doi.org/10.1111/j.1365-2435.2003.00790.x, 2003.

827 Serrano-Ortiz, P., Domingo, F., Cazorla, A., Were, A., Cuezva, S., Villagarcía, L., Alados-Arboledas,
828 L., Kowalski, A.S.: Interannual CO_2 exchange of a sparse mediterranean shrubland on a
829 carbonaceous substrate, J. Geophys. Res.: Biogeosci, 114, https://doi.org/Artn
830 G0401510.1029/2009jg000983, 2009.

831 Shen, R., Zhang, J.L., He, B., Li, F., Zhang, Z.M., Zhou, R., Ou, X.K.: The structure characteristic
832 and analysis on similarity of grassland community in dry-hot valley of Yuanjiang, Ecol. Environ.
833 Sci, 19, 2821−2825, https://doi.org/10.16258/j.cnki.1674-5906.2010.12.011, 2010.

834 Sulman, B.N., Roman, D.T., Yi, K., Wang, L.X., Phillips, R.P., Novick, K.A.: High atmospheric
835 demand for water can limit forest carbon uptake and transpiration as severely as dry soil,

Geophys. Res. Lett, 43, 9686–95, https://doi.org/10.1002/2016GL069416, 2016.

Sun, S.S., Wu, Z.P., Xiao, Q.T., Yu, F., Gu, S.H., Fang, D., Li, L., Zhao, X.B.: Factors influencing CO_2, fluxes of a grassland ecosystem on the Yunnan-Guizhou Plateau, China, Acta Prataculturae Sin, 29, 184–191, https://doi.org/10.7522/.10.11686/cyxb2019410, 2020.

Sha, Z.Y., Bai, Y.F., Li, R.R., Lan, H., Zhang, X.L., Li, J., Liu, X.F., Chang, S.J., Xie, Y.C.: The global carbon sink potential of terrestrial vegetation can be increased substantially by optimal land management, Commun. Earth Environ, 3, 8, https://doi. 10.1038/s43247-021-00333-1, 2022.

Tagesson, T., Fensholt, R., Cropley, F., Guiro, I., Horion., S. Ehammer. A., Ardö., J.: Dynamics in carbon exchange fluxes for a grazed semi-arid savanna ecosystem in West Africa, Agric. Ecosyst. Environ, 205, 15–24, https://doi.org/10.1016/j.agee.2015.02.017, 2015.

Taylor, P.G., Cleveland, C.C., Wieder, W.R., Sullivan, B.W., Doughty, C.E., Dobrowski, S.Z., Townsend, A.R.: Temperature and rainfall interact to control carbon cycling in tropical forests, Ecol. Lett. 20, 779–788, https://doi.org/ 10.1111/ele.12765, 2017.

Tarin, T., Nolan, R.H., Eamus, D., Cleverly, J.: Carbon and water fluxes in two adjacent Australian semi-arid ecosystems, Agric. For. Meteorol, 281, 107853, https://doi.org/10.1016/j.agrformet.2019.107853, 2020.

==Tang, J.W., Niu, B., Hu, Z.G., Zhang, X.Z.: Increasing susceptibility and shortening response time of vegetation productivity to drought from 2001 to 2021, Agric. For. Meteorol, 352, 110025, https://doi.org/10.1016/j.agrformet.2024.110025, 2024.==

Veenendaal, E.M., Kolle, O., Lloyd, J.: Seasonal variation in energy fluxes and carbon dioxide exchange for a broad-leaved semiarid savanna (Mopane woodland) in Southern Africa, Global Change Biol, 10, 318–328, https://doi.org/10.1111/j.1365-2486.2003.00699.x, 2004.

Weltzin, J.F., Loik, M.E., Schwinning, S., Williams, D.G., Fay, P.A., Haddad, B.M., Harte, J., Huxman, T.E., Knapp, A.K., Lin, G.H., Pockman, W.T., Shaw, R.M., Small, E.E., Smith, M.D., Smith, S.D., Tissue, D.T., Zak, J.C.: Assessing the response of terrestrial ecosystems to potential changes in precipitation, BioScience, 53, 941−952, https://doi.org/10.1641/0006-3568(2003)053[0941:ATROTE]2.0.CO;2, 2003.

Wen, X.F., Sun, X.M., Liu, Y.F., Li, X.B.: Effect of linear and exponential fitting on the initial rate of change in CO_2 concentration across the soil surface, Chin. J. Plant Ecol, 31, 380–385, https://doi.org/10.17521/cjpe.2007.0046, 2007.

Williams, A.P., Allen, C.D., Macalady, A.K., Griffin, D., Woodhouse, C.A., Meko, D.M., Swetnam, T.W., Rauscher, S.A., Seager, R., Grissino-Mayer, H.D., Dean, J.S., Cook, E.R., Gangodagamage, C., Cai, M., McDowell, N.G.: Temperature as a potent driver of regional forest drought stress and tree mortality, Nat. Clim. Change, 3, 292–297, https://doi.org/10.1038/nclimate1693, 2013.

Wang, W.Y., Guo, J.X., Wang, Y.S., Wu, K.: Observing characteristics of CO_2 flux and its influencing factors over Xilinhot grassland, J. Meteorol. Sci, 35, 100–107, https://doi.org/10. 3969 /2013jms. 0065, 2015.

Wu, F.T., Cao, S.K., Cao, G.C., Han, G.Z., Lin, Y.Y., Cheng, S.Y.: Variation of CO_2 flux of alpine wetland ecosystem of *Kobresta tibetica* wet meadow in Lake Qinghai, J. Ecol. Rural Environ, 34, 124–131, https://doi.org/10.11934/1.19n.1673-4831.2018.02.004, 2018.

Wang, N., Quesada, B., Xia, L.L., Butterbach-Bahl, K., Goodale, C.L., Kiese, R.: Effects of climate warming on carbon fluxes in grasslands – a global meta-analysis, Global Change Biol, 25, 1839–

1851, https://doi.org/10.1111/gcb.14603, 2019.

Wang, Y.Y., Xiao, J.F., Ma, Y.M., Luo, Y.Q., Hu, Z.Y., Li, F., Li Y.N., Gu, L.L., Li, Z.G., Yuan, L.: Carbon fluxes and environmental controls across different alpine grassland types on the Tibetan Plateau, Agric. For. Meteorol, 311, 1–14, https://doi.org/10.1016/j.agrformet.2021.108694, 2021.

Wang, F., Harindintwali, J.D., Wei, K., Shan, Y.L., Mi, Z.F., Costello, M.J., Grunwald, S., Feng, Z.Z., Wang, F.M., Guo, Y.M., Wu, X., Kumar, P., Kästner, M., Feng, X.J., Kang, S.C., Liu, Z., Fu, Y.H., Zhao, W., Ouyang, C.J., Shen, J.L., Wang, H.J., Chang, S.X., Evans, D.L., Wang, R., Zhu, C.W., Xiang, L.L., Rinklebe, J., Du, M.M., Huang, L., Bai, Z.H., Li, S., Lal, R., Elsner, M., Wigneron, J.P., Florindo, F., Jiang, X., Shaheen, S.M., Zhong, X.Y., Bol, R., Vasques, G.M., Li, X.F., Pfautsch, S., Wang, M.G., He, X., Agathokleous, E., Du, H.B., Kengara, F.O., Brahushi, F., Long, X.E., Pereira, P., Ok, Y.S., Rillig, M.C., Jeppesen, E., Barceló, D., Yan, X.Y., Jiao, N.Z., Han, B.X., Schäffer, A., Chen, J.M., Zhu, Y.G., Cheng, H., Amelung, W., Spötl, C., Zhu, J.K., Tiedje, J.M.: Climate change: Strategies for mitigation and adaptation, The Innovation Geosci, 1, 100015, https://doi. 10.59717/j.xinn-geo.2023.100015, 2023.

Williamson, G.J., Tng, D.Y.P., Bowman, D.M.J.S.: Climate, fire, and anthropogenic disturbance determine the current global distribution of tropical forest and savanna, Environ. Res. Lett., 19, 024032, https://doi.org/ 10.1088/1748-9326/ad20ac, 2024.

Wang, Z.K., Chen, W., Piao, J.L., Cai, Q.Y., Chen, S.F., Xue, X., Ma, T.J.: Synergistic effects of high atmospheric and soil dryness on record-breaking decreases in vegetation productivity over Southwest China in 2023, npj Clim Atmos Sci, 8, 6, https://doi.org/10.1038/s41612-025-00895-3, 2025.

Xiang, Y.B., Zhou, S.X., Xiao, Y.X., Hu, T.X., Tu, L.H., Huang, C.D.: Effects of precipitation variations on soil respiration in an evergreen broad-leaved forest during dry and wet seasons, Acta Ecol. Sin., 37, 4734−4742, https://doi.org/ 10.5846/stxb201604160701, 2017.

Xu, X.L: China watershed and river network datasets based on DEM extraction, Resource and Environmental Science Data Registration and Publishing System [data set], https://doi.org/10.12078/2018060101, 2018.

Xu, X.L: China's multi-year provincial administrative division boundary data, Resource and Environmental Science Data Registration and Publishing System [data set], https://doi.org/10.12078/2023010103, 2023a.

Xu, X.L: China's multi-year county administrative division boundary data, Resource and Environmental Science Data Registration and Publishing System [data set], https://doi.org/10.12078/2023010101, 2023b.

Yang, Z.P., Chang, Y.: Ecological problems of primary dry valleys is southwest China and advances in the researches into them, Agric. Res. Arid Areas, 25, 90−93, 2007.

Yu, K., D'Odorico, P.: Hydraulic lift as a determinant of tree–grass coexistence on savannas, New Phytol, 207, 1038–1051, https://doi.org/10.1111/nph.13431, 2015.

Yuan, W.P., Zheng, Y., Piao, S.L., Ciais, P., Lombardozzi, D., Wang, Y.P., Ryu, Y., Chen, G.X., Dong, W.J., Hu, Z.M., Jain, A.K., Jiang, C.Y., Kato, E., Li, S.H., Lienert, S., Liu, S.G., Nabel, J.E.M.S., Qin, Z.C., Quine, T., Sitch, S., Smith, W.K., Wang, F., Wu, C.Y., Xiao, Z.Q., Yang, S.: Increased atmospheric vapor pressure deficit reduces global vegetation growth, Sci. Adv, 5, eaax1396, https://doi.org/10.1126/sciadv.aax1396, 2019.

Yang, K.Y., Gong, H.D., Li, J., Liu, Y.T., Sha, L.Q., Song, Q.H., Jin, Y.Q., Yang, D.X., Li, P.G., Wen,

G.J., Chen, A.G., Pang, Z.Q., Zhang, Y.P.: Dynamic characteristics of soil respiration of savanna ecosystem in dry hot valley of Yuanjiang, J. Zhejiang Agric. For. Univ, 37, 849–859, https://doi.org/10.11833/j.issn.2095-0756.20190647, 2020.

Zhang, R.Z.: The dry valley of the Henduan Mountains region, Beijing Sci. Press, ISBN 703002916X, 1992.

Zhao, L., Gu, S., Xu, S.X., Zhao, X.Q., Li, Y.N.: Carbon flux and controlling process of alpine meadow on Qinghai-Tibetan plateau, Acta Botan. Boreali-Occidentalia Sin, 27, 1054–1060, 2007.

Zou, H., Gao, G.Y., Fu, B.J.: The relationship between grassland ecosystem and soil water in arid and semi-arid areas: a review, Acta Ecol. Sin, 36, 3127–3136, https://doi.org/10.5846/stxb201506211251, 2016.

Zhang, W.M., Brandt, M., Penuelas, J., Guichard, F., Tong, X., Tian, F., Fensholt, R.: Ecosystem structural changes controlled by altered rainfall climatology in tropical savannas, Nat. Commun, 10, 671, https://doi.org/10.1038/s41467-019-08602-6, 2019.

Zhang, R., Zhao, X.Y., Zuo, X.A., Qu, H., Degen, A.A., Luo, Y.Y., Ma, X.J., Chen, M., Liu, L.X., Chen, J.L.: Impacts of precipitation on ecosystem carbon fluxes in desert−grasslands in Inner Mongolia, China, J. Geophys. Res. Atmos, 124, 1266–1276, https://doi.org/10.1029/2018JD028419, 2019.

Zhao, H.C., Jia, G.S., Wang, H.S., Zhang, A.Z., Xu, X.Y.: Diurnal variations of the carbon fluxes of semiarid meadow steppe and typical steppe in China, Clim. Environ. Res, 25, 172–184, https://doi.org/10.3878/j.issn.1006-9585.2019.19096, 2020.

Zhang, Y.J., Qiu, L.P., Gao, H.L., Liu. J., Wei, X.R., Zhang, X.C.: Responses of ecosystem CO_2 exchange to clipping in a semi-arid typical grassland on the Loess Plateau, Acta Ecol. Sin, 40, 336–344, https://doi.org/10.5846/stxb201810172244, 2020.

Zeng, Z.Q., Wu, W.X., Li, Y.M., Huang, C., Zhang, X.Q., Peñuelas, J., Zhang, Y., Gentine, P., Li, Z.L., Wang, X.Y., Huang, H., Ren, X.S., Ge, Q.S.: Increasing meteorological drought under climate change reduces terrestrial ecosystem productivity and carbon storage, One Earth, 6, 1326–1339, https://doi.org/10.1016/j.oneear.2023.09.007, 2023.

Zhou, Y., Bomfim, B., Bond, W.J., Boutton, T.W., Case, M.F., Coetsee, C., Davies, A.B., February, E.C., Gray, E.F., Silva, L.C.R., Wrigh, J., Staver, A.C.: Soil carbon in tropical savannas mostly derived from grasses, Nat. Geosci, 16, 710−716, https://www.nature.com/articles/s41561-023-01232-0, 2023.